Technical Note N-1178

SEAFLOOR PENETRATION TESTS: PRESENTATION AND ANALYSIS OF RESULTS

By

H. J. Migliore and H. J. Lee

August 1971

Approved for public release; distribution unlimited.

NAVAL CIVIL ENGINEERING LABORATORY
Port Hueneme, California 93043

SEAFLOOR PENETRATION TESTS: PRESENTATION AND ANALYSIS OF RESULTS

Technical Note N-1178

YF 38.535.002.01.009

by

H. J. Migliore and H. J. Lee

ABSTRACT

A series of eleven in situ penetration tests was conducted by the Naval Civil Engineering Laboratory (NCEL) at two seafloor sites. The objectives of these tests were to illustrate the capabilities of existing penetration evaluation equipment and to acquire data for use in evaluating a series of proposed penetration prediction techniques. The tests consisted of allowing two types of objects to free-fall into the seafloor with the accelerations experienced by the objects during penetration being recorded mechanically. The resulting data were subjected to a regression analysis which yielded information about the penetration mechanism but no practical results. This was followed by a physical analysis based on static soil mechanics relations. The latter analysis was shown to yield predictions of penetration depth which were within 50 percent of the measured values. A suggested prediction technique based on this analysis is presented.

AD 732 367

Unclassified

Security Classification

DOCUMENT CONTROL DATA - R & D

(Security classification of title, body of abstract and indexing annotation must be entered when the overall report is classified)

1. ORIGINATING ACTIVITY (Corporate author) Naval Civil Engineering Laboratory Port Hueneme, California 93043	2a. REPORT SECURITY CLASSIFICATION Unclassified 2b. GROUP

3. REPORT TITLE

SEAFLOOR PENETRATION TESTS: PRESENTATION AND ANALYSIS OF RESULTS

4. DESCRIPTIVE NOTES (Type of report and inclusive dates)

Not final; December 1969-July 1970

5. AUTHOR(S) (First name, middle initial, last name)

H. J. Migliore and H. J. Lee

6. REPORT DATE	7a. TOTAL NO. OF PAGES	7b. NO. OF REFS
August 1971	60	12

8a. CONTRACT OR GRANT NO. b. PROJECT NO. YF 38.535.002.01.009 c. d.	9a. ORIGINATOR'S REPORT NUMBER(S) TN-1178 9b. OTHER REPORT NO(S) (Any other numbers that may be assigned this report)

10. DISTRIBUTION STATEMENT

Approved for public release; distribution unlimited.

11. SUPPLEMENTARY NOTES	12. SPONSORING MILITARY ACTIVITY
	Naval Facilities Engineering Command

13. ABSTRACT

A series of eleven in situ penetration tests was conducted by the Naval Civil Engineering Laboratory (NCEL) at two seafloor sites. The objectives of these tests were to illustrate the capabilities of existing penetration evaluation equipment and to acquire data for use in evaluating a series of proposed penetration prediction techniques. The tests consisted of allowing two types of objects to free-fall into the seafloor with the accelerations experienced by the objects during penetration being recorded mechanically. The resulting data were subjected to a regression analysis which yielded information about the penetration mechanism but no practical results. This was followed by a physical analysis based on static soil mechanics relations. The latter analysis was shown to yield predictions of penetration depth which were within 50 percent of the measured values. A suggested prediction technique based on this analysis is presented.

DD FORM 1 NOV 65 1473 (PAGE 1)

S/N 0101-807-6801

Unclassified

Security Classification

64

Unclassified

Security Classification

14. KEY WORDS	LINK A		LINK B		LINK C	
	ROLE	WT	ROLE	WT	ROLE	WT
Penetration tests						
Sediments						
Ocean bottom						
Measuring instruments						
Rheological properties						
Acceleration (physics)						
Regression analysis						
Marine geology						
Predictions						
Forecasting						
Soil mechanics						

DD FORM 1 NOV 68 1473 (BACK)
(PAGE 2)

Unclassified

Security Classification

CONTENTS

INTRODUCTION

Object penetration into the seafloor is an important mechanism occurring in many Naval undersea operations. For example, whenever a seafloor structure is placed, the foundation will penetrate the seafloor to some extent. In some instances, including pile and embedment anchor installation, it will be desirable to obtain large penetration, while in other instances, including spread footing placement, it will generally be desirable to minimize penetration behavior of the foundation.

Other situations in which seafloor penetration plays a major role are search and salvage operations involving missing or sunken ships and ordnance. When Naval equipment is lost and presumed to be embedded in the seafloor, it is of value to be able to predict possible ranges of embedment depths so that the nature of the search mission can be planned accordingly.

Another important application of seafloor penetration involves the use of penetrators, dynamic or static, to measure soil engineering properties. Such devices as these might eventually become among the most economical tools for obtaining large quantities of soil information for use in site selection or the design of small foundations. However, the mechanism of seafloor penetration must be better understood before such pieces of testing equipment can be used effectively.

On the basis of these applications, several research projects have been sponsored by the Navy to develop better techniques for predicting and utilizing seafloor penetration.

BACKGROUND

The Naval Civil Engineering Laboratory (NCEL) has pursued several projects related to the penetration problem. In early efforts, the major emphasis was directed toward static penetration. A seafloor plate bearing device and a static cone penetrometer were developed and tested at various seafloor locations off the coast of California. The results of these tests were analyzed and techniques for using the results were developed and presented in technical reports.[1,2]

Vibratory and explosive embedment anchors which utilize the penetration mechanism as means of installation have also been developed by NCEL.[3,4] Some penetration data have been acquired with these devices and analyzed, but the full potential of this equipment as a means for investigating penetration has not as yet been realized.

Seafloor penetration in general was discussed in some detail in two state-of-the-art contract reports funded by NCEL. In one of these reports,[5] authored by Dr. W. E. Schmid of Princeton University, the existing techniques for analyzing and predicting object penetration are presented and discussed. It is concluded that much of the past research involving high speed ballistic penetration of soil and other materials is not directly applicable to seafloor penetration. The equations which have been developed are empirical and contain coefficients which reflect the characteristics of high speed penetration but do not consider the unique properties of soft seafloor soils. The limited work which is applicable to seafloor penetration is considered next, and several closed-form equations for the penetration of idealized objects (primarily spheres) into homogeneous materials with combined velocity-dependent and static properties are developed. It is concluded that velocity dependent terms should be included in penetration prediction and that additional research is required to determine the characteristics of these terms. Some data for the low speed penetration of terrestrial soils are given, but virtually no data for seafloor penetration are provided.

In the other state-of-the-art report,[6] authored by Dr. R. J. Smith of the Naval Postgraduate School, a brief review of past penetration research is also included. Most of the report is concerned with a statement of the technique currently used by the Navy to predict object penetration. This technique involves a step-by-step numerical solution based on work-energy concepts. Forces acting upon an object during penetration are calculated using classical static soil mechanics equations evaluated in terms of static soil properties. No data are included to verify the technique.

As a result of this previous work and the subsequent conclusion that seafloor penetration is not currently well understood, NCEL, under the sponsorship of the Naval Facilities Engineering Command, initiated in 1969 a study of the physical processes involved. The objective of this study is to develop capabilities to predict the penetration behavior of any object given object configuration, soil properties and boundary conditions.

This report considers an initial phase of the study, a limited series of in situ penetration tests which were conducted during December 1969. Free-fall penetration was selected for investigation in these tests because it is a form which is relatively easy to analyze, existing equipment could be used, and the results could be applied toward a number of seafloor engineering problems.

OBJECTIVES

The objectives of this report are (1) to present the results of a series of in situ penetration tests, (2) illustrate the capabilities of existing penetration evaluation equipment, (3) discuss the value

of several different analytic techniques, and (4) recommend the technique which predicts the measured data best.

APPROACH

The approach used in this in situ testing program was first to acquire previously developed accelerometer, penetrometer, and coring equipment. Second, a two day cruise aboard a Navy YFU was conducted, soil cores were taken, and free-fall cone penetrometer tests performed. The accelerometer was mounted on the equipment during both operations thereby allowing all tests to be utilized as penetration tests. Two test sites in the Santa Barbara Channel off Southern California were investigated. Next, the soil samples obtained were subjected to a series of laboratory index property and shearing resistance tests. The accelerometer records were reduced and a preliminary analysis was performed. Two analytic techniques were used: (1) a regression analysis of the accelerometer records was performed in an attempt to derive soil property information and (2) the measured soil property information was used in a physical analysis in an attempt to synthesize the accelerometer records. Conclusions based on these analyses were drawn, and recommendations for future investigations were developed.

TEST EQUIPMENT

The acceleration data used in this penetration investigation were acquired with a Scott Accelerometer, developed for use in analyzing the behavior of seafloor gravity corers.[7] The accelerometer is a self-contained unit which is mounted atop a corer or penetrometer to measure the acceleration of the package. The main components are batteries, a governed motor, a rotating drum, and a moving stylus (see Figure 1). The motor rotates two components: the drum and a worm gear. The worm gear gives the stylus a downward motion parallel to the axis of the drum. A piece of recording paper is fastened to the drum and the paper is marked by the stylus. Consequently, the marked line reflects two motions, the drum rotation and the stylus motion parallel to the drum axis. However, the rotating drum is mounted on a spring and damper. The drum represents the mass in a spring-mass-damper system where any net acceleration on the drum would result in a commensurate motion. Therefore, in the case of zero net acceleration (constant velocity), the marked line would be a result of drum rotation and stylus motion, solely, and would have the form of a simple helix. In the case of non-zero acceleration (changing velocity), the drum would also move on its spring-damper supports and the marked line would deviate from the form of a helix. This deviation is a measure of the acceleration.

The overall packaging of the accelerometer and corer/penetrometer was developed by W. L. Preslan of the University of Delaware.[8] Figure 2 shows the overall configuration of the device which included a lifting eye, weights, a case for the accelerometer, a "quick change" mechanism for accommodating either the corer or penetrometer, and, in this particular photograph, the penetrometer. The dimension from the top of the eye to the bottom of the accelerometer case is 62 inches. The accelerometer case is 7 inches in outside diameter and the weights are 15 inches in outside diameter. The penetrometer is an inverted cone with a base of 2 inches and a height of 2 inches and is attached to a 74-inch-long, 1-inch-O.D. shaft. The corer is a 69-inch-long tube with a 3.25-inch-O.D. and a 3.00-inch-I.D. The mass of the corer and penetrometer is approximately 5.4 slugs.

TESTING PROGRAM

During December 1969, NCEL performed two series of coring and penetration tests. The two test sites were at depths of approximately 120 feet (Pitas Point Site) and 1200 feet (1200-Foot Site), (see Table 1). The corer/penetrating device was connected to a lowering line by a triggering mechanism of the type usually used in oceanographic coring. The triggering mechanism was activated by a 20-foot line extending below it. The device was lowered to within 20 feet of the bottom by the ship's winch, where the triggering mechanism was activated, thus allowing the corer/penetrometer to free-fall into the seafloor. The tests also included a timing mechanism because of the limited recording capacity of the accelerometer. The commencement of recording had to be delayed, by this timer, at the 1200-Foot Site to ensure that the final portion of the test would be recorded.

SOIL TESTS

A series of standard soil index property tests was performed on the soil samples obtained at each site for soil classification purposes and for possible usage in future penetration test correlations. These results are summarized in Tables 2 through 7. In addition, a series of vane shear tests planned so as to indicate soil viscous effects was performed on the samples obtained. The speed of vane rotation was varied among four different rates from test to test. Plots of undisturbed and remolded strength versus depth for two rotation rates at each site are included in Figures 3 through 6. The order of testing was randomized so as to eliminate any overall differences between cores.

As may be seen there is a distinct rate effect for all cases. It is a stronger effect with undisturbed soil than with remolded soil, and it does not appear to increase significantly with soil strength.

The results are summarized in Figure 7 in which the undisturbed and remolded strengths averaged over the core lengths are plotted versus vane rotation rate. The general conclusions reached above are clearly illustrated here.

DATA REDUCTION AND RESULTS

The first step in the data reduction process involved the photographic enlargement of the accelerometer record for increased clarity. For some tests the free-fall penetration region was interrupted by the seam of the paper. Data analysis was simplified by cutting and repiecing the plot paper so that the photo showed the free-fall and penetration as a continuous line.

The next phase of data reduction involved digitizing the plot. The purpose was to have a series of coordinated points which represent the plot. The discrete values could then be used in a digital computer program for further analysis. The digitizing device was essentially a measuring device which gave the coordinates of a selected point from a reference point. The operator looked through an aiming device at the photographically enlarged record and arbitrarily selected points on the plot by depressing a button. The reference point was established at the end of the penetration. The operator followed the plot from the reference point in the aimer and selected various points by depressing the button. This sampling scheme of various coordinated points described that particular plot. The coordinate values for each point were recorded as five-place integers on computer punch cards and typed out on paper tape by the digitizer. These integers were related to acceleration and time values by a computer program.

The computer program had two salient functions. One was to read the digitized data and make the conversion of coordinate values to acceleration and time values. Also, the program had to compensate for the helical nature of the output. This compensation was necessary because a simple helix transforms into an inclined straight line when the plot paper is unfolded from the drum. A correction factor was incorporated in the program to account for this inclination in the reference line, in effect, converting the output from "helical coordinates" to rectilinear coordinates. The second function involved the numerical integration of the acceleration to obtain velocity and displacement. The plots were approximated by fitting linear segments between each digitized point and integrated by summing the various areas under these straight lines. Some inaccuracy was introduced since the actual plot between any two points was not a straight line. However, close digital sampling over the entire curve had a tendency to "average out" any differences and thus mitigate the error. The typical digital output included time increments (dictated by the digital sampling increments), acceleration increments, velocity increments (integration of acceleration), displacement increments (integration of velocity), and force increments (the mass of the entire object times the acceleration). Plotting subroutines were then used to transform the digital results back into continuous plots.

In most tests, the identification of soil entry was difficult to determine. The technique used was to examine the forces on the object in the water as opposed to the forces on the object in the soil. A plot of velocity-squared versus acceleration is necessary, and its rationale begins with the following hydrodynamic force equations.[8]

$$(m + c)\, a = -mg \left(\frac{\rho_c - \rho_w}{\rho_c}\right) + C_D \left(\frac{\rho_w}{2}\right) A_p v^2 \qquad (1a)$$

$$a = -\left(\frac{mg}{m + c}\right) \left(\frac{\rho_c - \rho_w}{\rho_c}\right) + \left(\frac{C_D}{m + c}\right) \left(\frac{\rho_w}{2}\right) A_p v^2 \qquad (1b)$$

where a = acceleration, feet per second per second

g = acceleration of gravity, feet per second per second

m = the mass of the object, slugs

ρ_c = the average mass density of the object, slugs per cubic foot

ρ_w = the mass density of water, slugs per cubic foot

C_D = coefficient of drag, dimensionless

A_p = profile area, square feet

v = velocity, feet per second

c = "added mass" associated with accelerating water around an object, slugs

The left hand side of Equation 1a represents the net force on the object (ma) plus the "added mass" associated with accelerating an object through a fluid. The first term on the right is buoyancy and weight lumped together to represent the driving force. The second term is the drag force.

By dividing through by $(m + c)$, Equation 1b is derived. The form of the relation between a and v^2 is a straight line with slope, $\frac{C_D}{(m + c)} \frac{\rho_w}{2} A_p$ and acceleration intercept, $-\frac{mg}{(m + c)} \frac{\rho_c - \rho_w}{\rho_c}$.

Figure 8 shows a plot of velocity squared versus acceleration for a typical penetrometer test. When extra-hydrodynamic forces are acting on the object, such as those encountered in penetrating the seafloor, the plot will deviate from the hypothetical straight line. The right loop of the graph represents the straight-line hydrodynamic region, and the gross deviation of the left loop represents the object penetrating the soil. Consequently, a velocity-squared or acceleration value at the point of deviation may be used as a mark to distinguish the solely water data and the water-soil data (penetration data). The sign convention of Figure 8, and subsequent plots, is positive acceleration downward.

Ostensibly, the right loop of the test plots does not represent a straight line. The reasons for the error are two-fold. One, the paying of the retrieval line introduced unsteady decelerations as represented by the oscillating plot. Two, the non-zero start is a residual error resulting from integration, calibration, and ship motion. The numerical integrations begin at the end of the penetration test (where acceleration is known to be zero). Consequently, the error accumulates and manifests itself as residual velocity at the beginning of free-fall. Also, the modulus of the drum spring is not a constant and is approximated bilinearly; therefore, the conversion from drum movement to acceleration values contains a small error. Lastly, ship and winch line movement impart an initial velocity which is recorded in the initial free-fall measurements. In many of the tests, the oscillatory error caused by the above factors did not camouflage the gross deviation occurring at the soil-water interface. In some tests, however, it was difficult to discern the one oscillation that marked soil entrance.

The results of the penetration data reduction are shown in Table 8. Figures 9 through 12 are acceleration versus soil depth plots for the two test sites, showing the similar objects on the same graph.

ANALYSIS

General

The limited field and laboratory testing program which has been described yielded detailed penetration records in the form of deceleration versus soil depth plots (Figures 9 through 12) and a set of soil property data for each of the two sites investigated. It was the intention of the analysis phase of this investigation to present techniques for relating these two forms of data and thereby to suggest approaches for:

(1) Predicting penetration response given the soil characteristics at a site; and

(2) Predicting the soil properties at a site given the results of a penetration test.

Approaches of these types would be of value in planning and executing seafloor operations and in designing penetrators for use as seafloor survey tools.

The analysis of the data, therefore, was divided into two general areas. In the first, the accelerometer records were analyzed statistically using regression analysis in an attempt to derive general parameters which would be representative of soil and penetrator characteristics. In the second area of analysis, the soil and penetrator characteristics were inserted into several rational penetration equations, and the resulting theoretical acceleration versus depth plots were compared with the actual measured accelerometer data. The results of these two analyses are included in the following sections and a discussion of the implications of the results is included in the DISCUSSION section.

Regression Analysis

Using the procedure outlined in the REDUCTION discussion, acceleration, velocity, and displacement were calculated for each test. Also, each set of test data was divided into a water region and a soil penetration region. The next phase of the investigation was to develop a means to evaluate the data.

The approach that was employed was to examine the forces acting on the object and develop an appropriate force equation. The basic equation of interest was that forces on the object must equal the mass of the object times its acceleration. The question then arises, which forces are acting on the object? Solely in the water, there are two: driving force (buoyancy and weight lumped together) and drag force. As the object enters the soil, however, there are various soil forces encountered in addition to the solely water forces (hydrodynamic forces). These soil forces include wall friction, frontal resistance and inertial forces.

$$\Sigma F = ma = F_D + F_H + F_{SW} + F_{SF} + F_I \qquad (2)$$

where F = force, pounds

m = mass, slugs

a = acceleration, feet per second per second

F_D = driving force which reflects the weight of object and the buoyancy of the object in water

F_H = water drag force on the surface of the object

F_{SW} = frictional force on the walls of the object produced by the soil

F_{SF} = resistance force encountered by the front of the object as it moves through the soil

F_I = force produced in accelerating the fluid or soil around the object

In the first phase of the analysis, equations involving powers of velocities and displacements were assumed as approximate representations of Equation 2. These were in turn analyzed statistically to determine which constant parameters would cause the proposed equations to fit the data best. The forms of the equations were determined by assuming the nature of the forces acting on the object. For example, a general penetration equation should contain pure hydrodynamic forces. These would take the form of a constant force due to weight and buoyancy and a velocity-squared term due to water drag. As the testing device enters the soil, additional forces are encountered, such as viscous resistance of the soil (a function of velocity) and soil shear strength which changes with depth of penetration (a function of displacement). The form of the first proposed equation was as follows:

$$F_{net} = (m + c)\, a = A' + B'v^2 + C'v + D'x \qquad (3a)$$

where F_{net} is net force on object

m = mass of object

c = "added mass"

a = acceleration

v = velocity

x = displacement (penetration)

A', B', C', D' = coefficients reflecting physical factors

This force equation can be transformed into an acceleration equation:

$$a = A + Bv^2 + Cv + Dx \qquad (3b)$$

where $A = A' /(m + c)$

$B = B' /(m + c)$

$C = C' /(m + c)$

$D = D' /(m + c)$

A digital computer program was available to perform a regression analysis on the proposed equation[9]. Since the data were available in digital form, it was an easy matter to input values of acceleration and respective velocity, velocity-squared, and displacement for each of the tests. The output of the regression analysis consisted of values for the coefficients, A, B, C, and D and statistical information for each test.

After performing the regression analysis, Equation 3b was found to be a weak duplication of the test data. Consequently, several other euqations were proposed and analyzed until reasonable correlation resulted. The following equations were analyzed, in succession, and were all found to have weak correlation:

$$a = A + Bv + Cx \tag{4}$$

$$a = A + Bv^2 + Cv + Dx + Fvx + Fx^2 \tag{5}$$

$$a = A + Bv^2 + Cv + Dx + Exv + Fx^2 + Gv^3 + Hv^3x \tag{6}$$

$$a = A + Bv^2 + Cv + Dx + Exv + Fx^2 + Gv^3 + Hx^3 + Iv^4 \tag{7}$$

Equation 8 was found to duplicate the data from any given test with high correlation:

$$a = A + Bv^2 + Cv + Dx + Evx + Fx^2 + Gv^3 + Hx^3 + Iv^4 + J(vx)^2 + K(vx)^3 \tag{8}$$

Because of the complexity of Equation 8 and because the regression analysis revealed that several terms were insignificant, a modification to Equation 8 was formulated and analyzed. Its form was:

$$a = A + Bv^2 + C(vx) + D(v^2x) \tag{9}$$

(It should be emphasized that even though the constant coefficients, A, B, etc., appear several times in the above equations, these coefficients do not symbolize the same value from equation to equation.) The results of the regression analysis on Equation 9 were as follows:

Test Number	Object Type	Coefficients				Correlation Coefficients
		A	B	C	D	
PT1	Corer	-2.39	-0.004	0.89	0.05	.82
PT2	Corer	-3.37	0.06	0.35	-0.04	.95
PT3	Cone	-3.35	-0.01	2.75	0.18	.98
PT4	Cone	2.67	0.02	1.85	0.12	.99
PT5	Cone	0.56	-0.04	2.43	0.13	.97
PT6	Corer	-1.94	0.05	0.61	0.04	.96
PT7	Corer	-0.58	0.05	2.27	-0.14	.99
PT9	Cone	-1.94	0.09	1.40	0.10	.98
PT11	Corer	-1.36	0.02	0.65	0.02	.98
PT12	Corer	-0.98	-0.02	1.14	0.06	.98

Since Equation 9 represented the test data (with a slightly higher correlation than Equation 8), it was the final form to be tested in a regression analysis.

In Equation 9, as in Equations 3 through 8, all the force terms were selected by predicting the form of pertinent forces acting on the object as it penetrates. Equation 9 most accurately correlates to the actual test data, and its form represents the penetration phenomena for this series of tests. However, it is evident that some discrepancy exists in the assigned coefficients of the equation. Similar tests should have similar coefficient values, but they are different. The conclusion is that this regression analysis has only supplied a possible form of the force equation. A somewhat modified approach would be necessary in order to achieve a usable penetration equation, and this was pursued, as described in the following sections.

Physical Analysis

As discussed above in the BACKGROUND section, most of the existing penetration prediction techniques are not applicable to the case of seafloor penetration. The techniques of Schmid[5] may be applicable to the idealized situations considered but require considerable

modification for use with (1) a soil with properties which vary with depth and (2) irregularly-shaped objects. Only a numerical technique such as that of Smith[6] appears to be directly applicable to these more general situations. However, the technique of Smith should be modified somewhat to more accurately model the penetration process. Several additional force terms should be considered, and the relationship for predicting the penetrating object frontal resistance should be modified.

The proposed modified prediction technique is based upon Equation 2:

$$\Sigma F = ma = F_D + F_H + F_{SW} + F_{SF} + F_I \tag{2}$$

where the terms are as defined previously. Considering each term separately and defining downward forces as positive:

1. F_D - The driving force is equal to the weight of the object in water.

2. F_H - The hydrodynamic drag force is usually expressed by an equation of the form:

$$F_H = -C_D \rho_w \frac{v^2}{2} Ap \tag{10}$$

where C_D = drag coefficient

ρ_w = mass unit weight of water

v = object velocity

A_p = object cross-sectional area perpendicular to motion

For a given object the drag equation may be written more simply as

$$F_H = -D_s v^2 \tag{11}$$

where D_s = specific drag coefficient

For the two objects tested, the parameter D was obtained empirically from the accelerometer data corresponding to the free-fall phase of the penetration experiments. The technique used may be seen by considering the complete equation of motion for an object falling through water:

$$(m + c)\, a = F_D - D_s v^2 \qquad (12)$$

where c = added mass (included to account for F_I)

F_D = driving force = buoyant weight of object = W_b

If v^2 is ploted versus a for the free-fall phase, it is seen that the slope of the curve will be $D/(m + c)$ and the intercept will be $W_b/(m + c)$.[8] Therefore, both c and D for the free-fall phase may be evaluated empirically. For the cone penetrator and the corer assemblies used in these tests the values of D and c obtained are as indicated in Table 9.

Table 9

Object	c	D_s
cone	1.0	0.39
core	1.0	0.25

(ft, lb, sec units)

It was assumed that both D and c remained constant after the object entered the soil. This assumption ignores several features of penetration. For example, as an object penetrates the soil, less of the object is in contact with water, and it would be expected that the drag coefficient, D, would decrease in some complex manner. Likewise, since the unit mass of soil is greater than that of water and the soil flow mechanism is different from the water flow mechanism, it would be expected that the added mass, c, would vary in some undetermined manner as the object penetrates. For low velocity penetration such as that considered in these investigations, these aspects are probably relatively unimportant, and the assumption made is not unrealistic. For high speed penetration such an assumption would be totally unrealistic. Additional research is needed to evaluate these force terms for seafloor penetration.

3. F_{SW} - The soil side wall friction is evaluated in a manner identical to that of Smith[6]. This evaluation may be represented by the equation

$$F_{SW} = -\oint c_s \, dA_v \tag{13}$$

where c_s = soil unit shearing resistance produced along vertical surfaces of the object

dA_v = differential vertical surface area of object

It is somewhat difficult to determine exactly what values should be used for c_s. In some cases the soil will not be in contact with the object at every point, while in other cases the soil will be in contact but will be either practically undisturbed or totally remolded. In this analysis it was assumed that the soil was in contact with every vertical surface below the seafloor. For the low velocities involved this is probably a good assumption, but it is probably not applicable for very high velocity penetration. In terms of disturbance, two sets of calculations were performed, one using undisturbed or original strengths and the other, disturbed strengths. The strengths used were those obtained with the NCEL in situ vane device[2] at locations adjacent to the penetration test sites. Plots of these strengths are included in Figures 13 and 14. The linear fits of these data were used to simplify the integration of Equation 13. In compliance with the recommendations of Schmid[5], consideration was given to the effect which object velocity might have on soil shearing resistance. The preliminary soil tests indicated that shearing velocity might have a rather strong effect on the mobilized strength (Figures 3 through 7). Also the regression analysis indicated that velocity terms were quite important in determining the acceleration response. To incorporate time dependent shearing characteristics, the shear strength was allowed to vary with velocity as follows:

$$c_s = c_{so} + \mu v \tag{14}$$

where c_{so} = "static" soil strength (as measured in standard tests)

μ = soil viscosity coefficient

For the soils tested, values of μ were not known for the pertinent velocity ranges. Therefore, several values of μ were randomly selected and inserted in the equations to determine what sorts of results they would yield. The values of μ used were 0, 0.5, 1.0, and 3.0 lb-sec/ft^3.

4. F_{SF} - The frontal resistance force was evaluated by Smith[6] using shallow footing bearing capacity equations. However, for most cases of penetration, including the tests reported herein, the usage of such equations for the entire penetration process is not justified. This is because shallow footing equations degenerate as the penetration depth becomes large relative to the least lateral dimension of the penetrometer.[10] For these tests with long slender objects, the point of equation degeneration occurs early in the penetration process. The case then becomes one of "deep penetration" which is more appropriately predicted using pile bearing capacity equations. The frontal resistance force portion of these equations is usually represented by

$$F_{SF} = - \oint N c_s dA_h \tag{15}$$

where N = frontal pressure coefficient (>1.0)

c_s = soil shearing strength

dA_h = differential horizontal surface area of object

For piles placed in a cohesive soil medium, values of N which are used typically range between 7 and 9.5[5,6], a value of 10.0 was used in this investigation somewhat arbitrarily as a simple, reasonable number. Once again remolded and undisturbed values of c_s were used as were the previously stated four values for μ.

5. F_I - The technique for predicting the inertial force is incorporated in the technique discussed above for predicting the hydrodynamic drag force. This force is considered by introducing the added mass, c.

The final form of the penetration equation is as follows:

$$(m + c)\, a = W_b - Dv^2 - \oint c_s dA_v - \oint 10 c_s dA_H \tag{16}$$

where c_s is evaluated using Equation 14.

This equation was solved approximately by the following numerical procedure:

The object velocities at soil entry were known for all of the in situ penetration tests. For a given test the value of entry velocity and a penetration depth of zero were inserted into Equation 16.

The acceleration, a, at entry was then calculated. The velocity and penetration depth at Δt seconds after soil entry were calculated according to the relations

$$v_{\Delta t} = v_o + a\Delta t \tag{17}$$

$$x_{\Delta t} = x_o + \left(\frac{v_{\Delta t} + v_o}{2}\right) \Delta t \tag{18}$$

where v_o = entry velocity

$v_{\Delta t}$ = velocity after Δt seconds

x_o = entry penetration depth (=0)

$x_{\Delta t}$ = penetration depth after Δt seconds

A new value of acceleration, a, was then calculated and the iterative process continued. The completion of penetration was taken as the point at which the velocity became equal to zero.

This procedure would converge to an exact solution as Δt approached zero. In the calculations presented here, a value of Δt equal to .01 second was used. Other values of Δt were investigated to determine whether a solution based on this numerical procedure using this value of Δt would be stable. It was found that varying Δt between .025 second and .001 second altered the predicted ultimate penetration depth by only .3 percent. This was judged to be sufficiently accurate for the problem under consideration. All calculations were performed on a high speed computer.

The difference between this procedure and that of Smith[6] are as follows:

1. This procedure considers F_D, F_H, and F_I while Smith's does not.
2. This procedure uses a different relation for F_{SF}.
3. The numerical procedure used here involves an integration with respect to time while the Smith technique uses an integration with respect to penetration depth. Aside from the difference in force evaluation techniques, the two approaches would converge for Δt and Δx (penetration depth increment) approaching zero. However, for finite values of Δt and Δx, the solutions are probably somewhat different.

It should be noted that the technique used is a "pseudo-static" approach. Static soil bearing capacity equations are used, and all inertial effects are artificially incorporated into added mass and drag terms. This approach was used because existing equations could be used and little additional development was necessary. A better

approach and one which should be developed if more refined predictions are to be made would be a truly dynamic equation in which the dynamic characteristics are introduced rigorously.

The results of each penetration test were predicted using this technique. Since both disturbed and undisturbed soil characteristics and four values of soil viscosity coefficient, μ, were considered, a total of eight predictions were developed for each test. To minimize confusion the detailed results of only four test predictions will be presented. The results of the predictions for the other tests will be briefly summarized later.

The four tests selected for detailed presentation are PT-1, PT-4, PT-9, and PT-11. These tests include representatives of each object-site condition. The results are presented in Figures 15 through 18 in the form of predicted acceleration-depth plots compared with the measured curves. Each figure contains eight predicted curves and one measured curve.

Considering Figure 15 representing corer test PT-1 first, it is noted that the predicted curves involving remolded strengths with relatively small viscous coefficients (μ = 0.5-1.0 lb-sec/ft^3) predict the depth of penetration almost exactly. The curve with the high viscous coefficient (μ = 3.0 lb-sec/ft^3) and the undisturbed curves are much poorer in their capability to predict the penetration depth. However, none of the approaches actually predicts the shape of the acceleration-depth plot very well. The good penetration depth predictions achieved using remolded strengths with low viscosity may be purely coincidental.

In Figure 16 representing cone test PT-4, all of the predicted curves have shapes which approximate the measured curve. The prediction scheme which uses remolded strength and a soil viscosity coefficient, μ, of 1.0 yields the best prediction of penetration depth. All of the schemes, however, yield penetration depths which are within 20 percent of the measured depth.

In Figure 17 representing cone test PT-9, it is seen that the prediction scheme using remolded strength and low viscosity (μ = 0 - 0.5 lb-sec/ft^3) predicts the measured results almost exactly. The undisturbed and higher viscosity curves are considerably less accurate.

In Figure 18 representing corer test PT-11 the results are similar to those for PT-1. The remolded, low viscosity predicted curves are the most nearly accurate in terms of predicting penetration depth while none of the curves are particularly accurate in terms of reflecting the shape of the measured curves.

In the calculation of the predicted penetration behavior for the other tests, it was found that in all cases the shapes of the predicted cone penetratometer acceleration-depth plots agreed well with the shapes of the measured curves. The shapes of the predicted corer tests did not agree well. A comparison of the predicted penetration depths with the measured depths is presented in Table 10.

A careful examination of these data indicates that the best predictions for all except two tests are obtained with prediction schemes using remolded strengths. In terms of the importance of the viscosity parameter, μ, the results are inconclusive. Table 11, which presents the average percentage error produced with each scheme, illustrates some of the problems associated with determining the importance of soil viscosity. In terms of the overall average error, the scheme which uses remolded strengths and a soil viscosity of 3.0 appears to be most accurate. However, if the results listed in Table 10 are consulted again, it is seen that the schemes using lower viscosities (0.0 to 1.0 lb-sec/ft^3) are the most accurate for most of the tests. However they are greatly in error for tests PT-3 and PT-5. Since these tests were performed with the cone penetrometer, and since, owing to the small base area of this device, the soil entry point is difficult to determine, there is reason to believe that the original accelerometer records may have been misinterpreted. In any case the results of these tests conflict so strongly with the results and analyses of the other tests that there is a strong probability that an error or misinterpretation has been made somewhere in the data reduction process. Considering the average error resulting from the tests other than PT-3 and PT-5 as also presented in Table 10, it is seen that the scheme which uses remolded strength and the relatively small soil viscosity coefficient, μ, of 1.0 lb-sec/ft^3 yields the best results.

It should be noted, however, that all of these schemes yield relatively good penetration depth predictions. The scheme with the largest error is still within 50 percent of the correct solution. It may be concluded, therefore, that a penetration prediction scheme founded on "pseudo-static" concepts apparently yields good results for low velocity penetration. The use of remolded strength in the force prediction equations improves the prediction accuracy. The use of at least some modification for soil viscosity apparently produces greater accuracy. This is not a dominant factor, however.

DISCUSSION

The various results of the analysis and testing conflict somewhat. This is best illustrated by considering the following points:

1. The soil tests indicated a strong variation of shearing strength with shearing velocity.

2. The regression analysis indicated that velocity-dependent terms are the most significant in influencing penetration response.

3. The physical analysis indicated that static soil resistance altered only slightly to account for velocity dependency was most effective in predicting penetration response. The predictions obtained were rather good.

It should be noted that various aspects could have produced incorrect results in the regression analysis. For example, during the digitizing operation, points were sampled at approximately equal increments of time. Since the object travels faster when it first enters the soils than near the point of ultimate penetration, many more points were taken near the ultimate penetration point than near the point of entry into the seafloor. The regression equations, therefore, exaggerate the lower phases of penetration at the expense of the upper phases. The region in which the deceleration relaxes from its maximum point to zero (as clearly illustrated in Figures 9 through 12) is particularly exaggerated. This is a difficult region to analyze and it probably represents a phase in which the shearing resistance of the soil is not fully mobilized. An equation developed to fit both this region and the earlier regions in which the full shearing resistance almost certainly is mobilized has a strong probability of being somewhat in error.

Another problem inherent in the regression analysis is its failure to separate other phases of the penetration process. For example, at different penetration depths, different portions of the penetrators are embedded in the soil. Considering the cone penetrator, initially only the cone is embedded in the seafloor. This is followed by a long period in which the shaft following the cone becomes more and more deeply embedded. Finally, the housing for the accelerometer strikes the seafloor and becomes embedded. In the physical analysis, each of these phases is considered individually in the formulation of the area integrals. In the regression analysis all of the phases are masked together in one equation. The solution to this problem is to consider each phase of penetration separately and to derive separate regression equations for each. This should be undertaken in future penetration analyses. It is likely that more consistent, realistic regression coefficients will result.

Even if the conclusions based on the regression analyses are incorrect, the soil tests also yield results which conflict with the results of the physical analysis in terms of the importance of soil viscosity. For example, the slopes of the lines passing through the laboratory test data of Figure 7 yield values of viscosity coefficient, μ, ranging between 350 and 4000 lb-sec/ft^3 depending on which data are considered. The physical analysis, on the other hand, indicated that values of μ in the range of 0 to 3 lb-sec/ft^3 yielded the most accurate results. It is difficult to reconcile these differences on the basis of the limited tests which have been performed.

The basic problem, therefore, is exactly what role velocity-dependent terms or soil viscosity plays in affecting object penetration. This is not a purely academic question. If velocity-dependent terms are important, the problem of predicting penetration becomes significantly more complex. Penetration prediction schemes based on easily measured index properties would be difficult to develop if such a complex concept as soil viscosity needed to be considered. On the other hand,

if static terms are most significant the development of such a scheme could be relatively simple. Also, a survey penetrator would be of less value if the measured data included a complex combination of static and viscous quantities. More controlled research of the nature of that reported herein is required to determine more precisely what are the important factors affecting penetration.

SUGGESTED PREDICTION TECHNIQUE

Although there are presently many unanswered questions concerning the nature of the penetration mechanism, in practical situations it may be necessary to predict penetration responses before additional research can be performed. Therefore, one approach must be selected for use during this interim period. On the basis of the research and analyses presented above, it appears that the most accurate procedure currently available is a "pseudo-static" approach using remolded strengths. The slight additional accuracy brought about by the use of velocity-dependent soil resistance terms does not appear to be justifiable at present.

A procedure for using this approach in predicting penetration depth given entry velocity, soil strength profile, and object geometry, is presented below. The procedure could be inverted to yield soil strength characteristics given a penetration response.

1. The surface area of the object should be resolved into horizontal and vertical components. Progressing up the object from the bottom, the total horizontal and vertical surface area corresponding to each finite increment of object length should be calculated. A typical length increment, $\Delta\ell$, for a moderate size object would be perhaps six inches. For each increment the horizontal area should be multiplied by 10.0 and added to the vertical area. This is to account for the increased soil resistance encountered by horizontal surfaces. This sum is identified as the effective area coefficient A_e.

2. The effective area coefficient, A_e, should be tabulated as a function of the vertical distance from the bottom of the object.

3. An estimate of the remolded strength, c_s, versus sediment depth, ξ, should be made for the site. This may be obtained from laboratory tests on core samples, in situ tests, or through consultation with a soil engineer acquainted with the general area.

4. Estimate the object buoyant weight, W_b, the object mass, m, the added mass, c, and the specific drag coefficient, D_s $(=C_d \rho w \frac{A}{2} p)$. The latter two terms may be estimated for such objects as submarines through consultation with marine architects. If no estimate is possible, c may be assumed equal to zero and D_s equal to $\frac{W_b}{v_o^2}$ with no great loss in accuracy.

5. The entry velocity, v_o, if not known, should be estimated.

6. A value of time increment, Δt, for use in the finite difference evaluation should be established. An increment of .01 second was used in the analysis of the penetration tests presented in this report.

7. The Force, F, acting on the object at any depth, x, is calculated according to the equation

$$F = + W_b - D_s v^2 - \sum_{\xi=0}^{X} c_s (\xi) A_e (\ell) \qquad (19)$$

where $\ell = x - \xi$

$c_s(\xi)$ = soil strength as a function of ξ

$A_e(\ell)$ = effective area coefficient for zone $\ell - \frac{\Delta\ell}{2}$ to $\ell + \frac{\Delta\ell}{2}$

the summation is carried out at increments of ℓ and ξ equal to $\Delta\ell$. The calculation proceeds as follows:

a. The force corresponding to the initial velocity and zero embedment depth is calculated using Equation 19.

b. The entry acceleration, a, is calculated as $\frac{F}{m + c}$.

c. The velocity and embedment depth at the end of one time increment Δt are calculated using the relations:

$$v_{\Delta t} = v_o + a\Delta t \qquad (20)$$

$$x_{\Delta t} = x_o + \frac{v_{\Delta t} + v_o}{2} \cdot \Delta t \qquad (21)$$

d. The force corresponding to the new embedment depth and velocity is calculated (Equation 19).

e. The new acceleration is calculated.

f. The new velocity and embedment depth are calculated analogously to step (c) (Equations 20 and 21).

g. This iterative procedure continues until the velocity either equals 0 or becomes negative. The embedment depth corresponding to this situation is assumed to be the ultimate embedment depth.

SAMPLE PROBLEM

Consider a 10-foot diameter cylinder 30 feet in length with conical ends striking the seafloor vertically with the axis of the cylinder perpendicular to the seafloor. The altitudes of the conical ends are 10 feet. The entry velocity is 20 ft/sec, and it is assumed that this is the object terminal velocity. The object weighs 1000 pounds in water and has a mass of 5576 slugs. The remolded strength profile is given in Figure 20. (This is suggested as a typical profile for seafloor sites containing weak, cohesive soils.)

It is desired to calculate the ultimate depth of penetration.

1. From geometry, the distribution of horizontal and vertical area components are as given in the table below (taking $\Delta\ell = 0.5$ ft). The values of horizontal area, A_h, A_v, and A_e as functions of ℓ correspond to the section of object between $\ell + \frac{\Delta\ell}{2}$ and $\ell - \frac{\Delta\ell}{2}$. For example, the second increments of area (corresponding to $\ell = 0.5$) are calculated as follows:

The section is represented by a frustrum of a cone with the cross section:

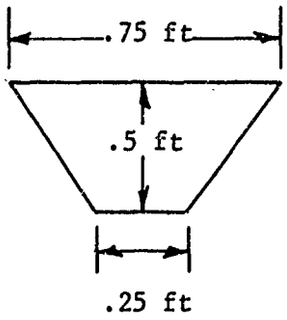

The vertical component of surface area is equal to the area of a cylinder having a radius equal to the average radius of the frustrum or in this case .5 ft.

$$A_v = \pi\ (.5)\ (.5)$$

$$= .7854\ ft^2$$

The horizontal component of area is equal to the horizontal projection of the curved surface of the frustrum.

$$A_h = \pi\ (\frac{.75}{2})^2 - \pi\ (\frac{.25}{2})^2$$

$$= .44178 - .04908$$

$$= .39370\ ft^2$$

$$A_e = A_v + 10A_h$$

$$= 4.7123$$

ℓ (ft)	A_h (ft^2)	A_v (ft^2)	A_e $(ft)^2$
0	.0491	.0982	.5892
0.5	.3927	.7854	4.7124
1.0	.7854	1.5708	9.4248
1.5	1.1781	2.3562	14.1372
2.0	1.5708	3.1416	18.8496
2.5	1.9635	3.9271	23.5620
⋮	⋮	⋮	⋮
10.0	3.8779	15.6027	54.3887
10.5	0	15.7079	15.7079
11.0	0	15.7079	15.7079
⋮	⋮	⋮	⋮

2. A_e is calculated and tabulated above.

3. The strength profile is given in Figure 20.

4. v_o = 20 ft/sec

5. $W_b = 1000$ lb

$$D_s = \frac{W_b}{v_1^2} = \frac{1000}{400} = 2.5 \frac{\text{lb-sec}^2}{\text{ft}^2}$$

Assume c = 0

6. Let $\Delta t = .01$ sec

7. a. $F = W_b - D_s v^2 - c_s(0)A_e(0)$

$= 1000 - 2.5\ (20)^2 - (20)\ (.5892)$

$= -11.784$ lb

b. $a = \frac{-11.784}{5576} = -.00212$ ft/sec^2

c. $v_{\Delta t} = 20 - (.00212)\ (.01)$

$= 19.999981$ ft/sec

$x_{\Delta t} = 0 + (20)\ (.01)$

$= .2$ ft

This completes the first iteration. In preparation for the second iteration, it is noted that the embedment depth after the first iteration is .2 feet. Since this is within the increment, $\Delta \ell = 0.5$ feet, centered about $\ell = 0$, the summation portion of the force equation still contains only one multiplication term. The calculation continues as follows:

d. $F = +1000 - 2.5\ (19.99998)^2 - (20)\ (.5892) = -13.5$ lb

e. $a = \frac{-13.5}{5576} = .00242$ ft/sec^2

f. $v_{2\Delta t} = 19.99998 - (.00242)\ (.01)$

$v_{2\Delta t} = 19.99995$ ft/sec

$x_{2\Delta t} = 0.2 + (\frac{19.999981 + 19.99995}{2})\ (.01)$

$= .40$ ft

This completes the second iteration. Since the new embedment depth is beyond the increment, $\Delta\ell$, centered about $\ell = 0$, two multiplication terms need to be included in the summation portion of the force equation. The calculation proceeds:

$$F = W_b - D_s (v_{2\Delta t})^2 - C_s (0) A_e (0.5) - c_s (0.5) A_e (0)$$

$$= 1000 - 2.5 (19.99995)^2 - (20) (4.7124) - (26) (.5892)$$

$$= -102.7 \text{ lb}$$

$$a = \frac{-102.7}{5576} = .01843 \text{ ft/sec}^2$$

$$v_{3\Delta t} = 19.99995 - (.01843) (.01)$$

$$= 19.99977 \text{ ft/sec}$$

$$x_{3\Delta t} = .40 + \left(\frac{19.99977 + 19.99995}{2}\right) (.01)$$

$$= .60 \text{ ft}$$

g. This iterative procedure was followed through 125 increments of Δt or 1.26 seconds of penetration time. At that point the velocity became negative and the corresponding embedment depth was assumed to be the point of maximum penetration. The penetration depth corresponding to this point was 17.8 feet. A summary of some of the intermediate results is given in the following table. The calculation procedure was simplified through the use of a brief computer code.

t (sec)	F (lb)	a (ft/sec^2)	v (ft/sec)	x (ft)
.00	0	.00000	20.00000	.00
.01	-11.8	-.00212	19.99998	.20
.02	-13.5	-.00242	19.99995	.40
.03	-102.7	-.01843	19.99977	.60
.04	-117.9	-.02115	19.99956	.80
.	.	.	.	.
.	.	.	.	.
.	.	.	.	.
.50	-58,079.6	-10.41600	18.48279	9.82
.51	-60,707.4	-10.88727	18.37392	10.01
.52	-63,091.8	-11.31490	18.26077	10.19
.	.	.	.	.
.	.	.	.	.
.	.	.	.	.
1.24	-181,453.9	-32.54195	.48407	17.79
1.25	-181,533.3	-32.55619	.15851	17.80
1.26	-181,559.1	-32.56083	-.16710	17.80

CONCLUSIONS

1. The penetration of objects into seafloor soils is a complex phenomenon which is poorly understood at present.

2. Complete tests in which all pertinent penetration characteristics are measured can yield valuable information which will be of assistance in ultimately developing valid penetration equations.

3. Regression analysis shows promise as a tool for determining which parameters are important and what the magnitude of the relevant coefficients should be. However, any regression analysis should be formulated carefully to include the physical characteristics of the problem.

4. A well-founded physical analysis based carefully upon engineering judgment appears to offer the most promise for immediate use in predicting penetration. In the analysis presented above, the use of what is basically a static pile bearing capacity equation in conjunction with a Newtonian equation of motion appeared to offer the most nearly accurate results.

5. The approach presented in the SUGGESTED PREDICTION TECHNIQUE section appears to be the most reasonable practical technique for use in the interim period before additional research is performed.

6. The effects of soil viscosity and penetrator velocity on object penetration are not well understood. The present investigation yielded conflicting results in this regard.

RECOMMENDATIONS

1. Additional complete investigations such as that reported herein are required for a better understanding of the penetration phenomenon.

2. This requirement can best be satisfied by the performance of a large number of laboratory penetration tests in which a variety of small penetrators are allowed to penetrate various simulated soils. It is imperative that each experiment be totally controlled. The motion of the penetrators as they penetrate should be accurately recorded either by means of an accelerometer or through photography. Soil properties should be accurately measured and controlled. The experiments should be designed statistically so that sahpe, velocity, size, and soil effects can be isolated.

3. The laboratory experiments should be supplemented by a limited series of in-situ tests of the nature of the tests described above only involving a greater variety of objects and entry velocities.

4. Analyses of the data obtained should include a regression analysis in conjunction with an improved physical analysis based on dynamic concepts.

5. Large-scale experiments conducted by the Navy which involve the sinking of large vessels should be carefully instrumented so as to yield as much information as possible on the penetration phenomenon. These should be supplemented by detailed tests of the surrounding seafloor soils.

6. Before the additional research is completed, the approach presented in the SUGGESTED PREDICTION TECHNIQUE section should be used for practical operations.

ACKNOWLEDGEMENT

The assistance provided by Dr. R. Scott and Dr. W. L. Preslan in planning and executing this investigation is gratefully acknowledged.

Table 1. Location and nature of tests

Test No.	Object	Location (degrees-minutes)		Depth (fathoms)
		Latitude	Longitude	
PT 1	Corer	34-16.93 N	119-23.98 W	19
PT 2	Corer	34-16.93 N	119-23.98 W	19
PT 3	Cone	34-16.93 N	119-23.98 W	19
PT 4	Cone	34-16.93 N	119-23.98 W	19
PT 5	Cone	34-16.93 N	119-23.98 W	19
PT 6	Corer	34-16.93 N	119-23.98 W	19
PT 7	Corer	34-16.93 N	119-23.98 W	19
PT 9	Cone	34-9.93 N	119-45.13 W	189
PT 11	Corer	34-9.05 N	119-44.48 W	200
PT 12	Corer	34-9.57 N	119-45.39 W	200

Table 2. Soil index properties - Pitas Point Site - Core PT 1.

Interval (in)	0-3	6-9	12-15	18-21	24-27	30-33
Bulk Wet Density (pcf)	96.	106.	105.	105.	104.	106.
Water Content (percent)	81.	57.	58.	57.	57.	54.
Specific Gravity of Solids	2.62	2.62	2.64	2.64	2.62	2.62
Dry Density (pcf)	53.	68.	67.	67.	66.	69.
Void Ratio	2.08	1.42	1.47	1.48	1.47	1.38
Liquid Limit (percent)	51.	43.	46.	44.	45.	42.
Plastic Limit (percent)	32.	28.	29.	28.	29.	30.
Plasticity Index	19.	15.	17.	16.	16.	12.
Liquidity Index	265.	191.	166.	177.	181.	200.
Sand (percent)	-	3.	-	1.	-	4.
Silt (percent)	-	67.	-	65.	-	65.
Clay (percent)	-	31.	-	34.	-	31.
Activity	-	.7	-	.7	-	.6
Median Diameter (mm)	-	.0122	-	.0097	-	.0126

Table 3. Soil index properties - Pitas Point Site - Core PT 2.

Internal (in)	0-3	6-9	12-15	18-21	24-27
Bulk Wet Density (pcf)	105.	103.	104.	106.	103.
Water Content (percent)	54.	60.	59.	55.	60.
Specific Gravity of Solids	2.63	2.63	2.63	2.61	2.61
Dry Density (pcf)	68.	64.	65.	68.	65.
Void Radio	1.41	1.55	1.52	1.38	1.52
Liquid Limit (percent)	38.	43.	45.	44.	47.
Plastic Limit (percent)	26.	28.	28.	28.	29.
Plasticity Index	12.	15.	17.	16.	18.
Liquidity Index	225.	212.	182.	171.	175.
Sand (percent)	-	3.	-	2.	-
Silt (percent)	-	68.	-	63.	-
Clay (percent)	-	29.	-	35.	-
Activity	-	.7	-	.7	-
Median Diameter (mm)	-	.0136	-	.0108	-

Table 4. Soil index properties - Fitas Point Site - Core PT 6.

Interval (in)	0-3	6-9	12-15
Bulk Wet Density (pcf)	103.	103.	103.
Water Content (percent)	58.	60.	60.
Specific Gravity of Solids	2.62	2.62	2.61
Dry Density (pcf)	65.	64.	64.
Void Ratio	1.51	1.55	1.54
Liquid Limit (percent)	46.	44.	47.
Plastic Limit (percent)	27.	31.	28.
Plasticity Index	19.	13.	19.
Liquidity Index	164.	218.	172.
Sand (percent)	-	2.	-
Silt (percent)	-	71.	-
Clay (percent)	-	27.	-
Activity	-	.7	-
Median Diameter (mm)	-	.0132	-

Table 5. Soil index properties - Pitas Point Site - Core PT 7.

Interval (in)	0-3	6-9	12-15	18-21	24-27	30-33
Bulk Wet Density (pcf)	101.	101.	103.	104.	107.	105.
Water Content (percent)	64.	61.	63.	61.	56.	60.
Specific Gravity of Solids	2.64	2.64	2.65	2.65	2.65	2.65
Dry Density (pcf)	61.	62.	63.	65.	69.	66.
Void Ratio	1.69	1.64	1.63	1.57	1.40	1.51
Liquid Limit (percent)	43.	47.	47.	44.	43.	47.
Plastic Limit (percent)	27.	30.	30.	29.	30.	29.
Plasticity Index	16.	17.	17.	15.	13.	18.
Liquidity Index	241.	188.	191.	213.	195.	173.
Sand (percent)	-	2.	-	2.	-	2.
Silt (percent)	-	67.	-	66.	-	61.
Clay (percent)	-	31.	-	32.	-	37.
Activity	-	.7	-	.7	-	.7
Median Diameter (mm)	-	.0113	-	.0110	-	.0091

Table 6. Soil index properties - 1200-Foot Site - Core PT 8.

Interval (in)	0-3	6-9	12-15	18-21	24-27
Bulk Wet Density (pcf)	78.	84.	87.	88.	88.
Water Content (percent)	191.	136.	125.	120.	121.
Specific Gravity of Solids	2.53	2.53	2.53	2.53	2.53
Dry Density (pcf)	27.	36.	39.	40.	40.
Void Ratio	4.92	3.42	3.08	2.94	2.93
Liquid Limit (percent	109.	100.	96.	101.	95.
Plastic Limit (percent)	47.	44.	45.	47.	48.
Plasticity Index	62.	56.	51.	54.	47.
Liquidity Index	230.	163.	156.	136.	154.
Sand (percent)	-	3.	-	1.	-
Silt (percent)	-	52.	-	53.	-
Clay (percent)	-	45.	-	46.	-
Activity	-	1.8	-	1.7	-
Median Diameter (mm)	-	.0068	-	.0060	-

Table 7. Soil index properties - 1200-Foot Site - Core PT 12.

Interval (in)	0-3	6-9	12-15	18-21	24-27	30-33
Bulk Wet Density (pcf)	78.	85.	85.	87.	89.	90.
Water Content (percent)	188.	139.	133.	125.	114.	108.
Specific Gravity of Solids	2.50	2.50	2.55	2.55	2.55	2.55
Dry Density (pcf)	27.	35.	36.	38.	42.	43.
Void Ratio	4.80	3.42	3.36	3.13	2.82	2.66
Liquid Limit (percent)	113.	107.	103.	108.	89.	93.
Plastic Limit (percent)	49.	47.	48.	50.	44.	47.
Plasticity Index	64.	60.	55.	58.	45.	46.
Liquidity Index	216.	155.	154.	128.	155.	133.
Sand (percent)	-	6.	-	3.	-	4.
Silt (percent)	-	48.	-	50.	-	51.
Clay (percent)	-	46.	-	47.	-	45.
Activity	-	2.0	-	1.7	-	1.5
Median Diameter (mm)	-	.0060	-	.0058	-	.0064

Table 8. Penetration test results.

Test	Shape	Water Depth (ft)	Acceleration at Seafloor Entry (ft/sec^2)	Velocity at Seafloor Entry (ft/sec)	Depth of Penetration (ft)
PT 1	Corer	114	6.14	14.46	6.86
PT 2	Corer	114	6.51	14.33	6.51
PT 3	Cone	114	2.79	14.25	5.92
PT 4	Cone	114	7.36	12.88	8.85
PT 5	Cone	114	4.92	14.52	5.69
PT 6	Corer	114	2.81	12.72	5.39
PT 7	Corer	114	8.81	11.98	5.29
PT 9	Cone	1134	9.09	10.22	8.95
PT 11	Corer	1200	3.83	15.56	8.41
PT 12	Corer	1200	1.44	17.64	8.17

Table 10. Predicted penetration depths.

Test Number	Measured Penetration Depth (ft)	Predicted Penetration Depths (ft)							
		Remolded Strength				Original Strength			
		$\mu = 0.0$	$\mu = 0.5$	$\mu = 1.0$	$\mu = 3.0$	$\mu = 0.0$	$\mu = 0.5$	$\mu = 1.0$	$\mu = 3.0$
PT 1	6.86	7.44	7.05	6.72	5.77	5.47	5.27	5.10	4.52
PT 2	6.51	7.43	7.03	6.70	5.77	5.45	5.25	5.08	4.51
PT 3	5.92	9.70	9.35	9.07	8.24	8.01	7.85	7.72	7.29
PT 4	8.85	9.58	9.24	8.97	8.17	7.88	7.74	7.60	7.20
PT 5	5.69	9.73	9.38	9.08	8.26	8.03	7.88	7.74	7.30
PT 6	5.39	7.18	6.81	6.50	5.56	5.18	5.01	4.83	4.29
PT 7	5.29	7.07	6.70	6.40	5.47	5.06	4.89	4.72	4.20
PT 9	8.95	8.73	8.50	8.30	7.70	7.31	7.20	7.10	6.77
PT 11	8.41	6.85	6.55	6.29	5.45	5.24	5.09	4.93	4.43
PT 12	8.17	7.14	6.82	6.54	5.70	5.70	5.37	5.21	4.67

Table 11. Accuracy of penetration prediction techniques.

Prediction Techniques	Average Error (%)	Average Error Excluding PT 3 and PT 5 (%)	Number of Tests Predicted Most Accurately with this Technique
Remolded Strength, $\mu = 0.0$	26.6	16.4	3
Remolded Strength, $\mu = 0.5$	23.4	14.0	0
Remolded Strength, $\mu = 1.0$	21.3	12.5	3
Remolded Strength, $\mu = 3.0$	20.5	15.1	2
Original Strength, $\mu = 0.0$	21.8	17.7	0
Original Strength, $\mu = 0.5$	23.4	20.4	0
Original Strength, $\mu = 1.0$	24.8	22.7	0
Original Strength, $\mu = 3.0$	28.9	29.6	2 (PT 3 and PT 5)

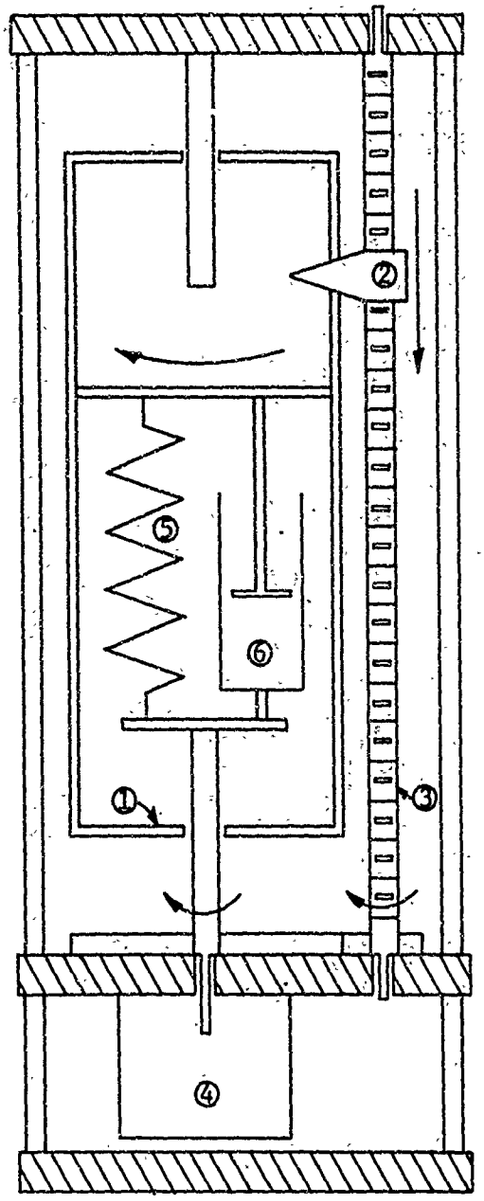

Figure 1. Schematic view of Scott Accelerometer[8] (Patent pending by Dr. R. F. Scott) (©University of Delaware. Used by permission.)

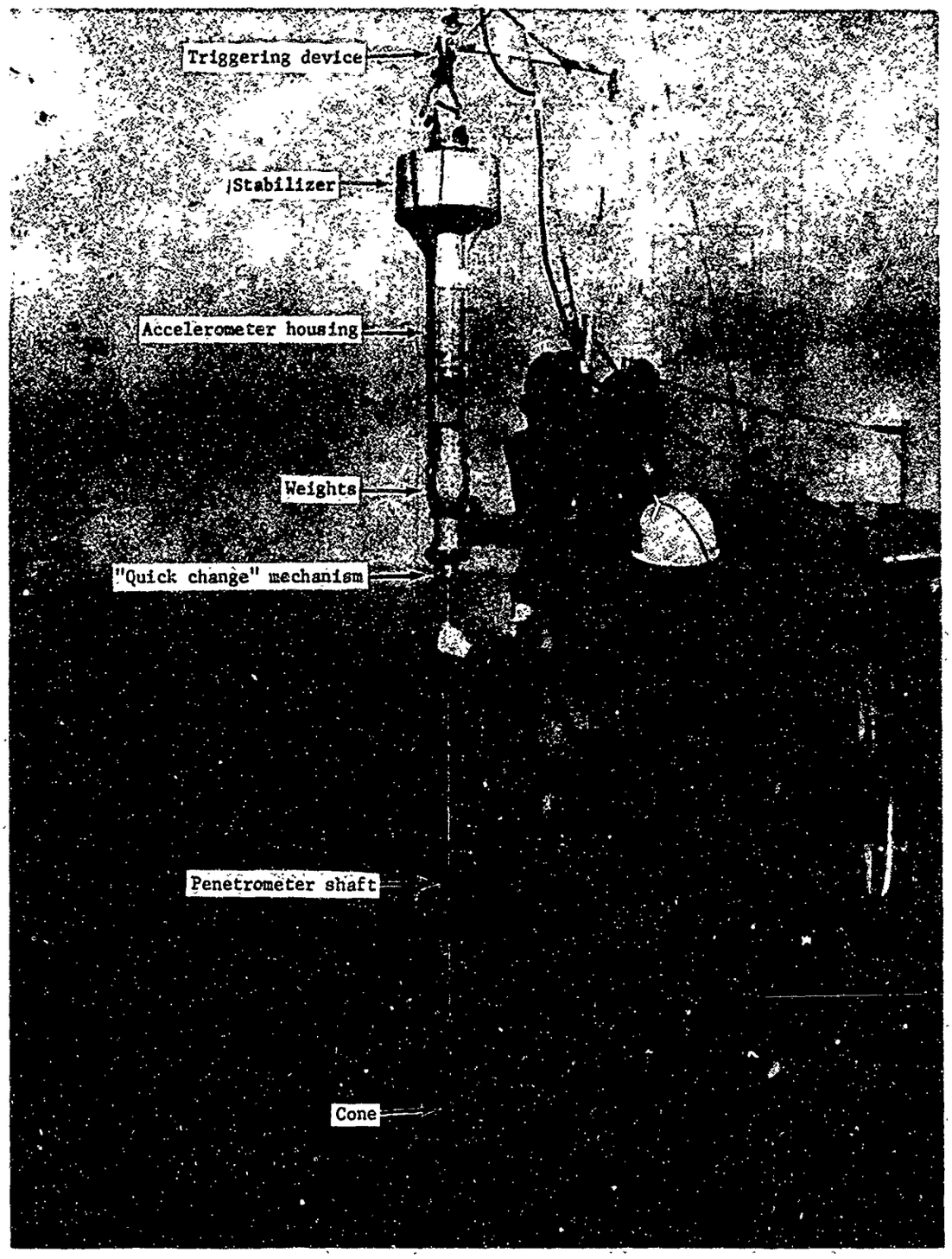

Figure 2. Penetrometer package.

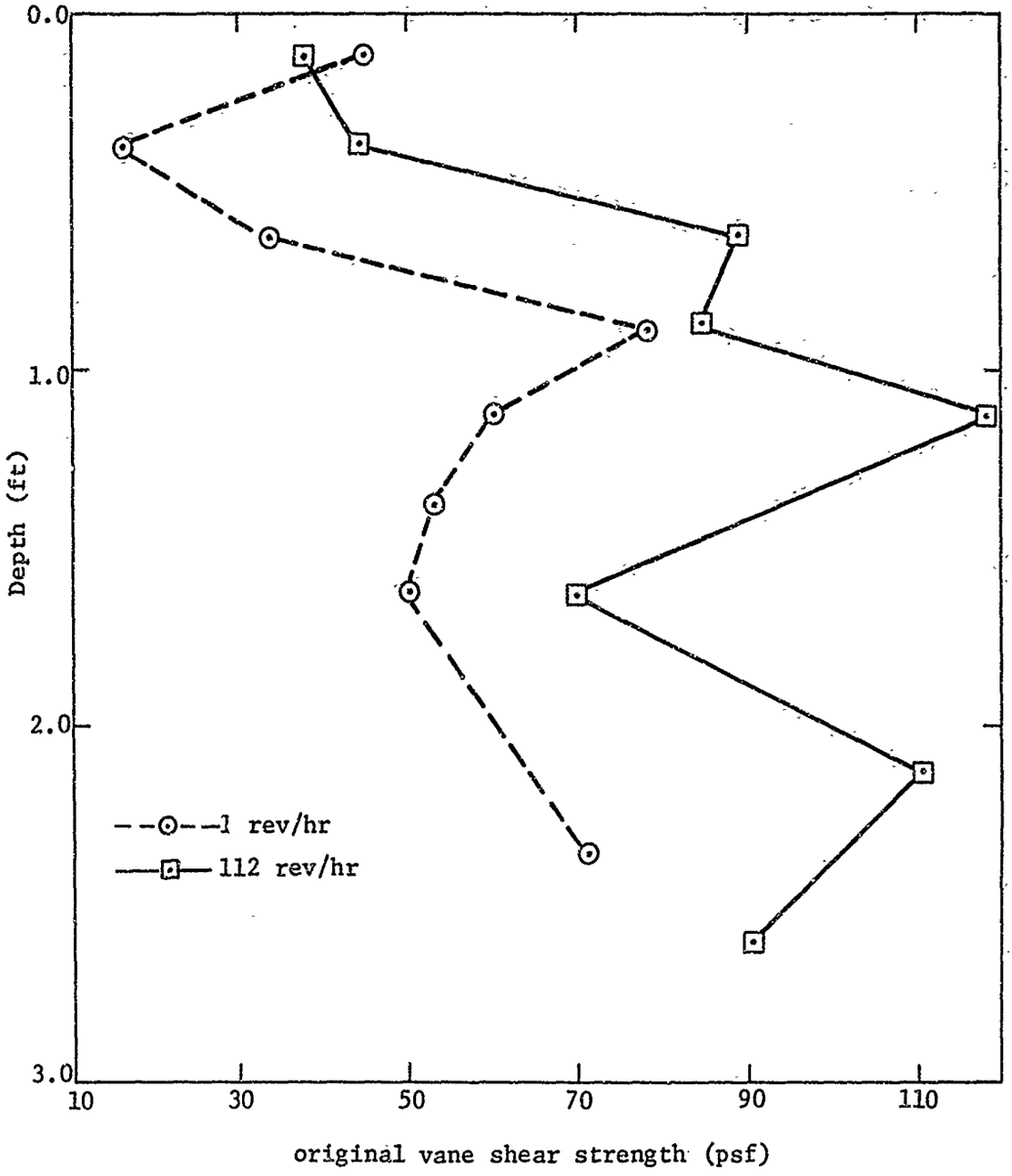

Figure 3. Original strength versus depth at Pitas Point Site for two vane rotation rates (1-inch diameter vanes used).

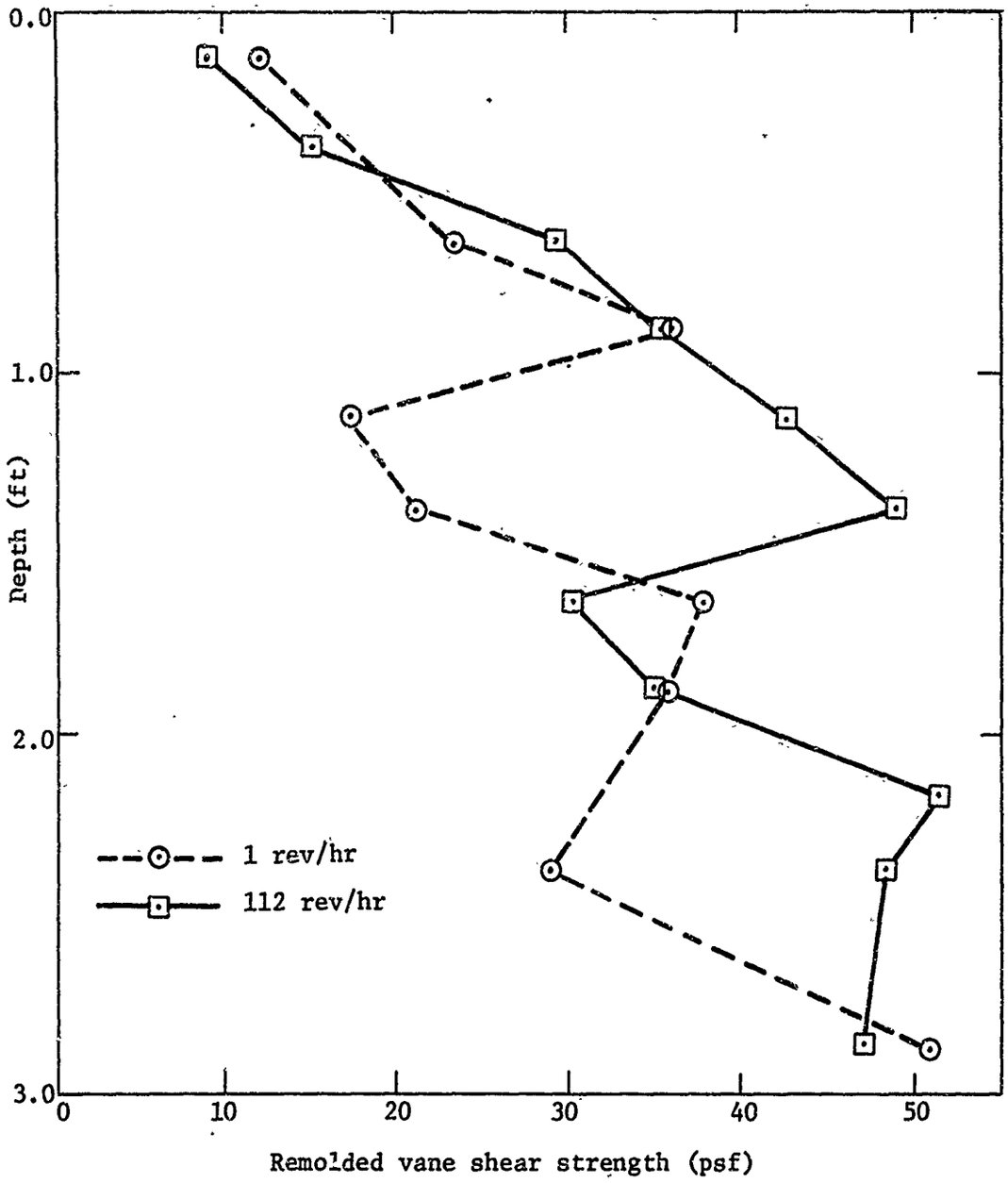

Figure 4. Remolded strength versus depth at Pitas Point Site for two vane rotation rates (1-inch diameter vane used).

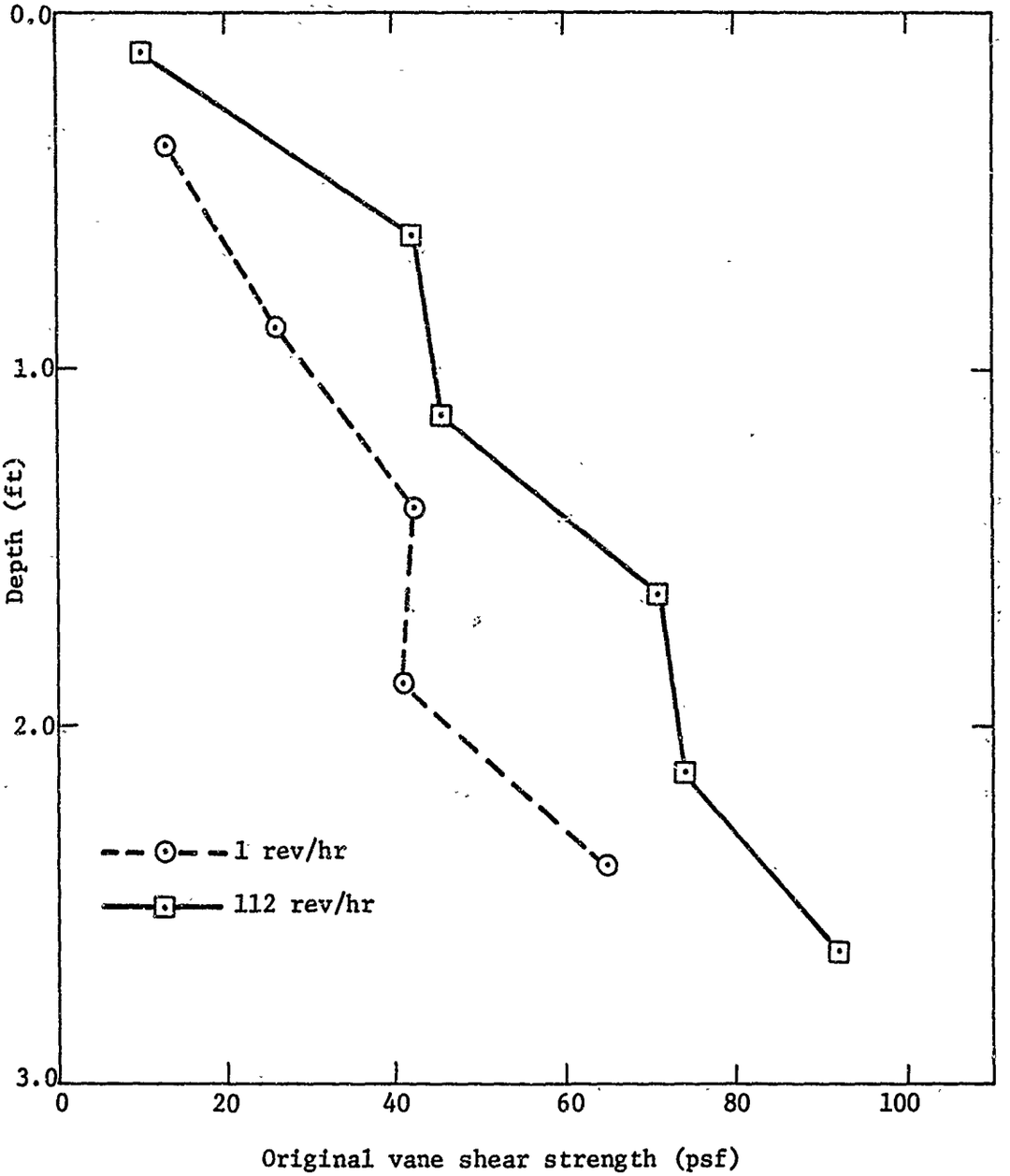

Figure 5. Original strength versus depth at 1200-Foot Site for two vane rotation rates (1-inch diameter vanes used).

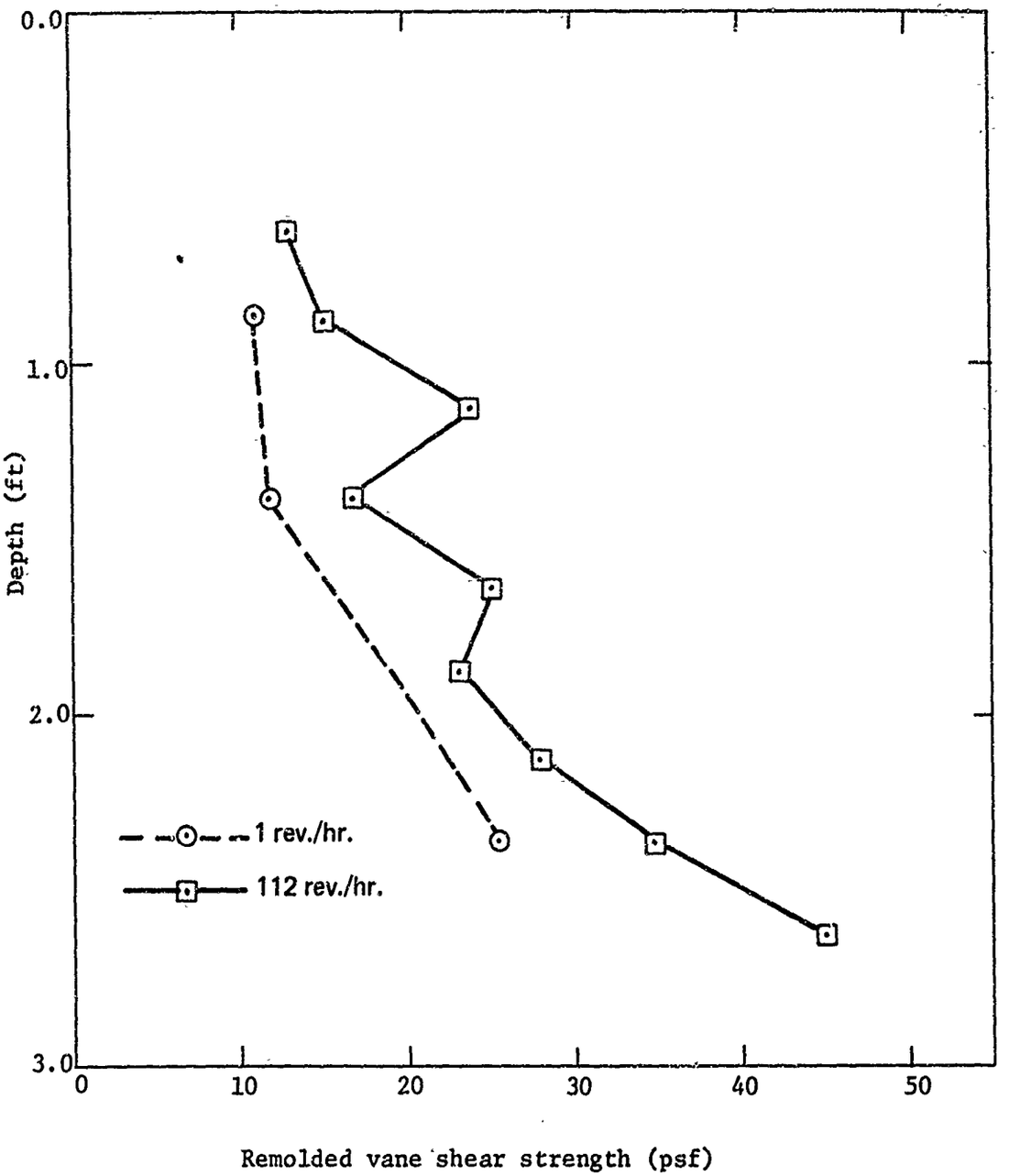

Figure 6. Remolded strength versus depth at 1200-Foot Site for two vane rotation rates (1-inch diameter vanes used).

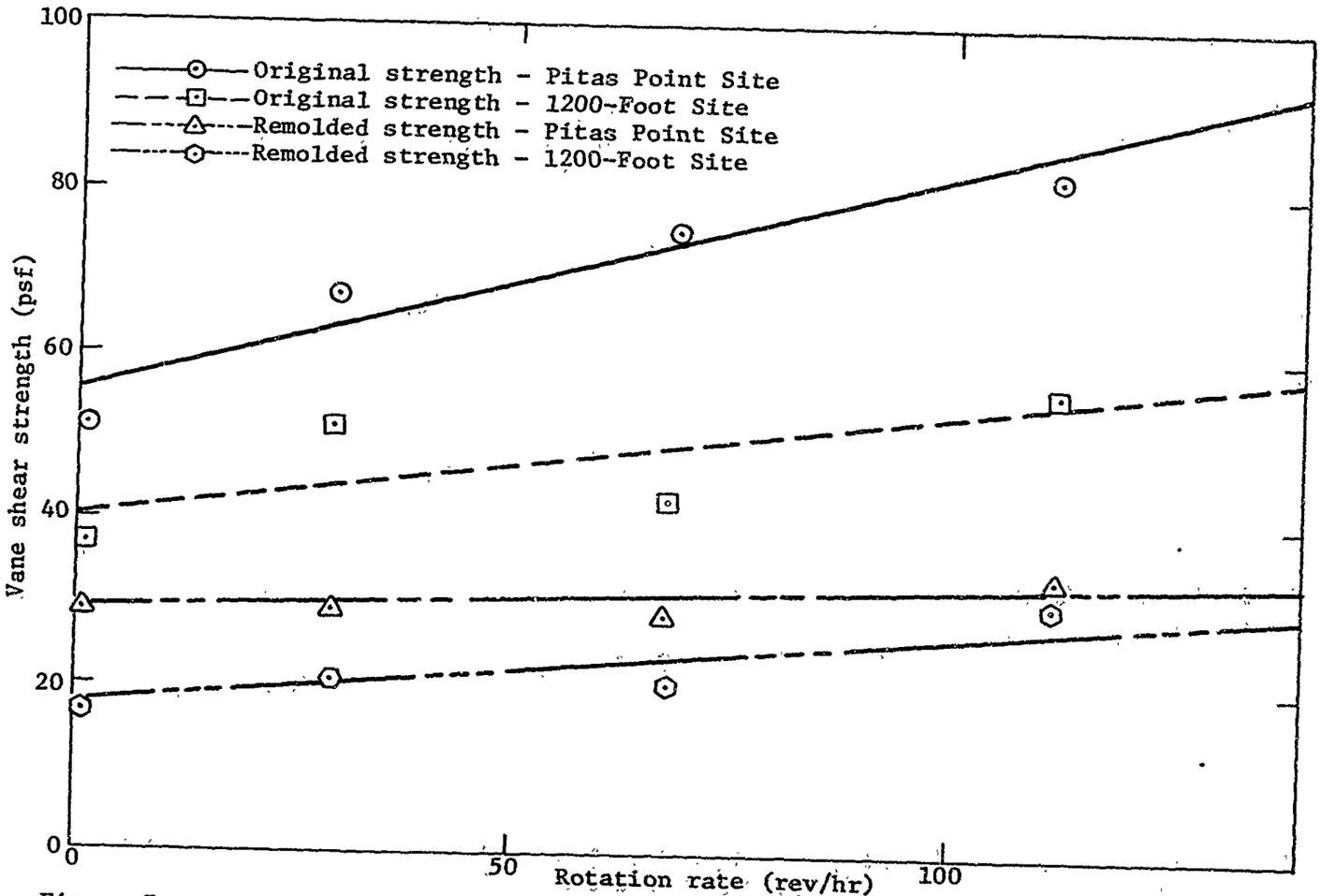

Figure 7. Average original and remolded vane strength versus vane rotation rate - Pitas Point and 1200-Foot Sites (1-inch diameter vane used).

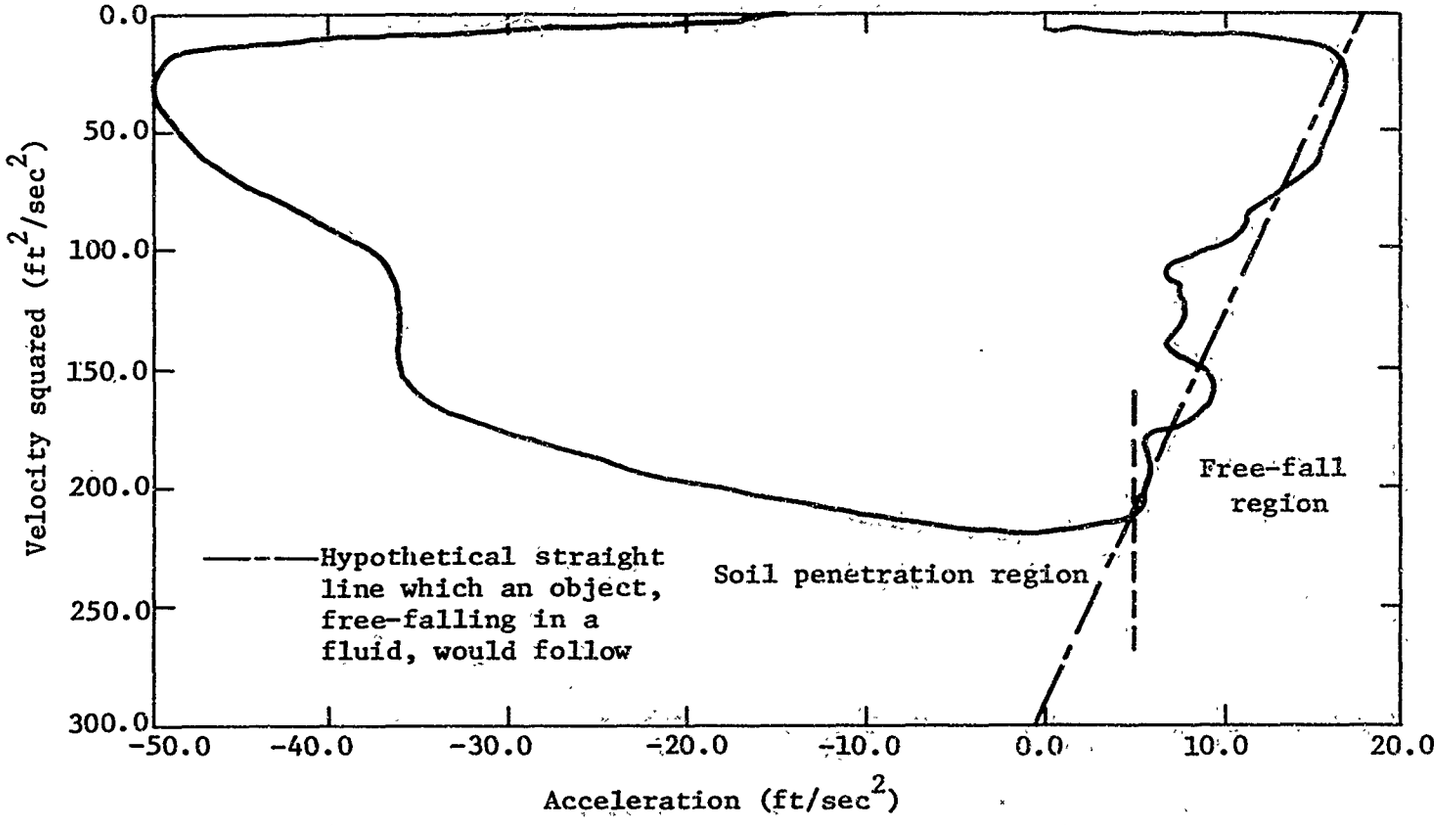

Figure 8. Velocity-squared versus acceleration for a typical penetrometer test (PT 5).

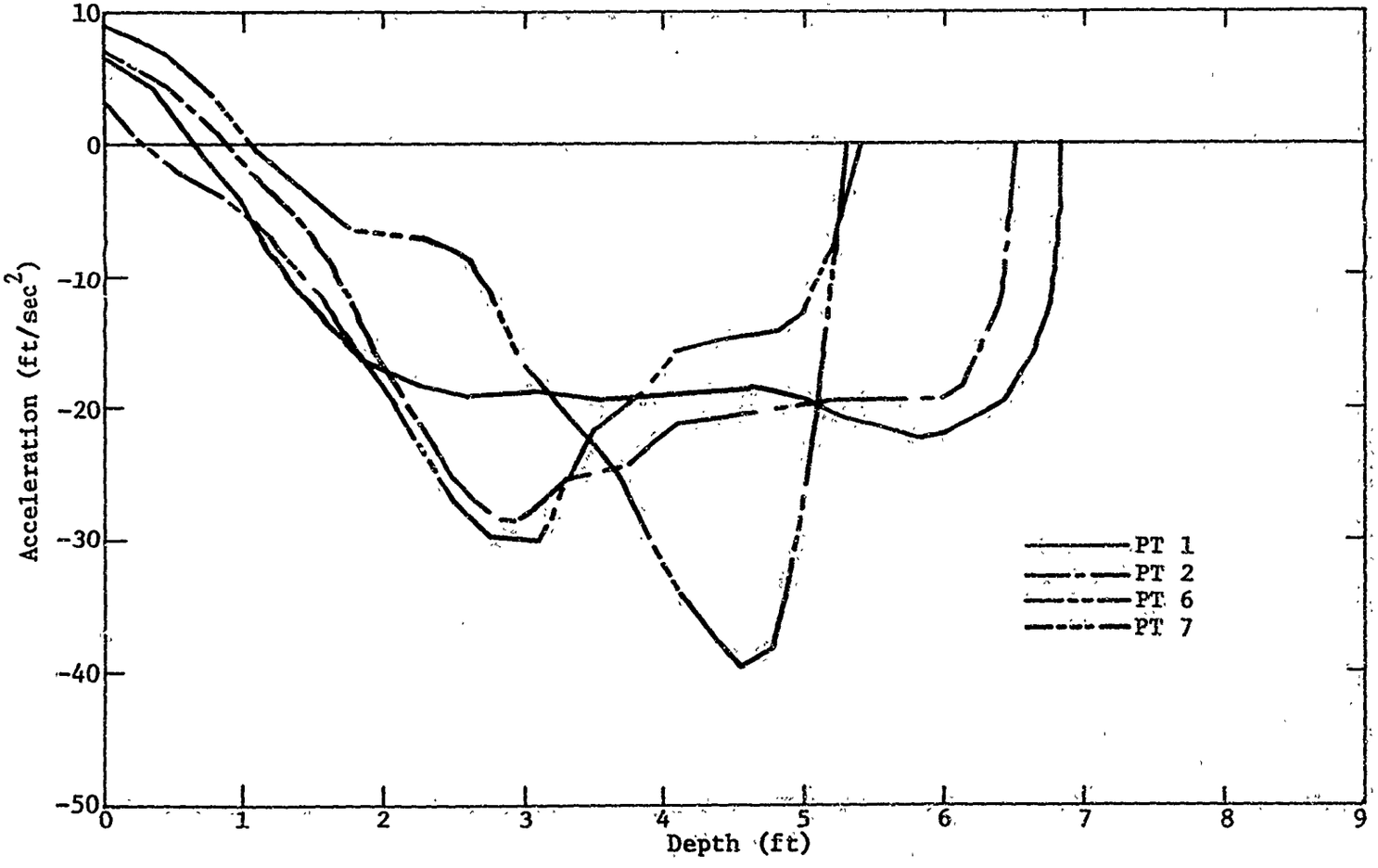

Figure 9. Acceleration versus depth - coring tests at Pitas Point Site.

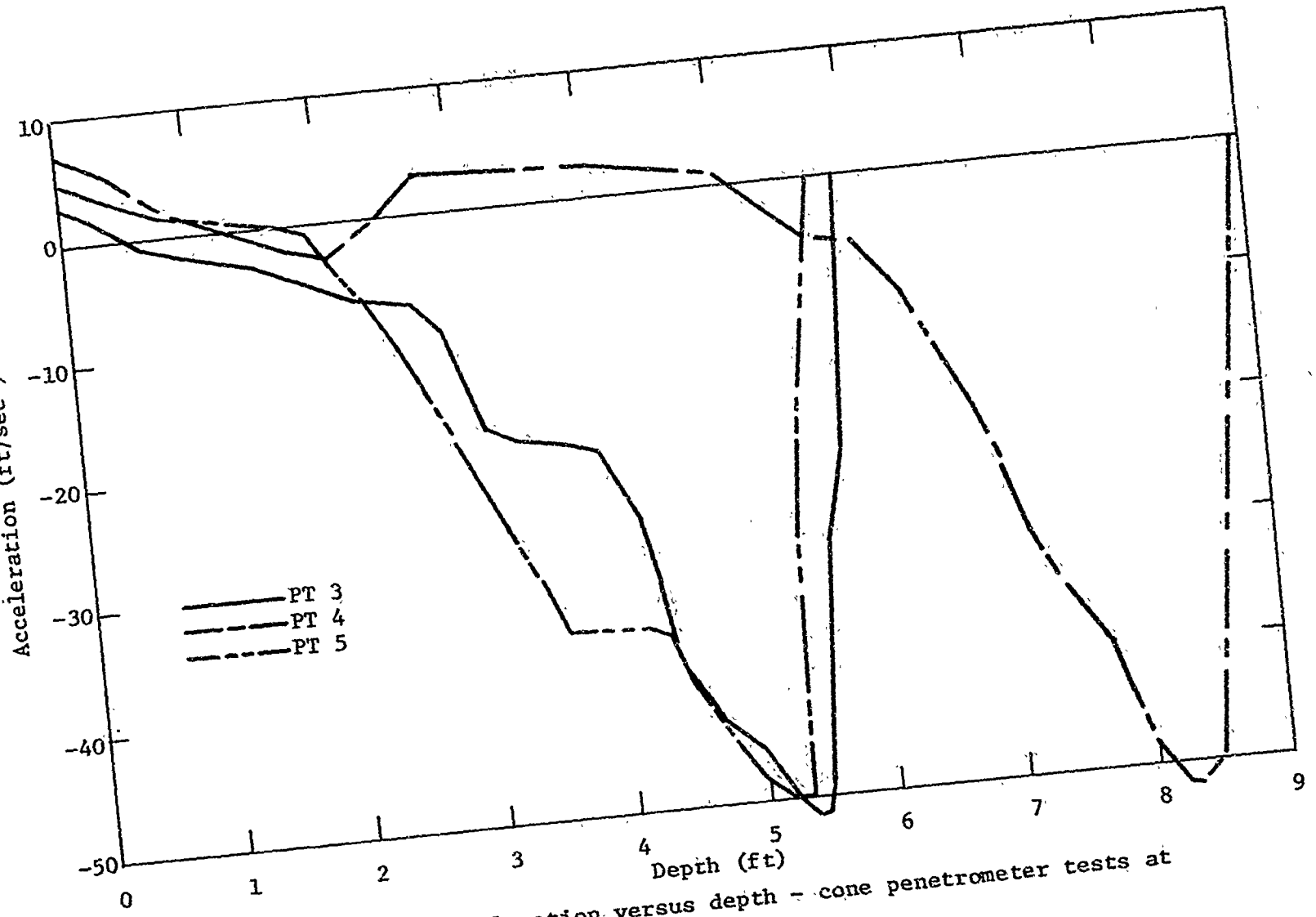

Figure 10. Acceleration versus depth - cone penetrometer tests at Pitas Point Site.

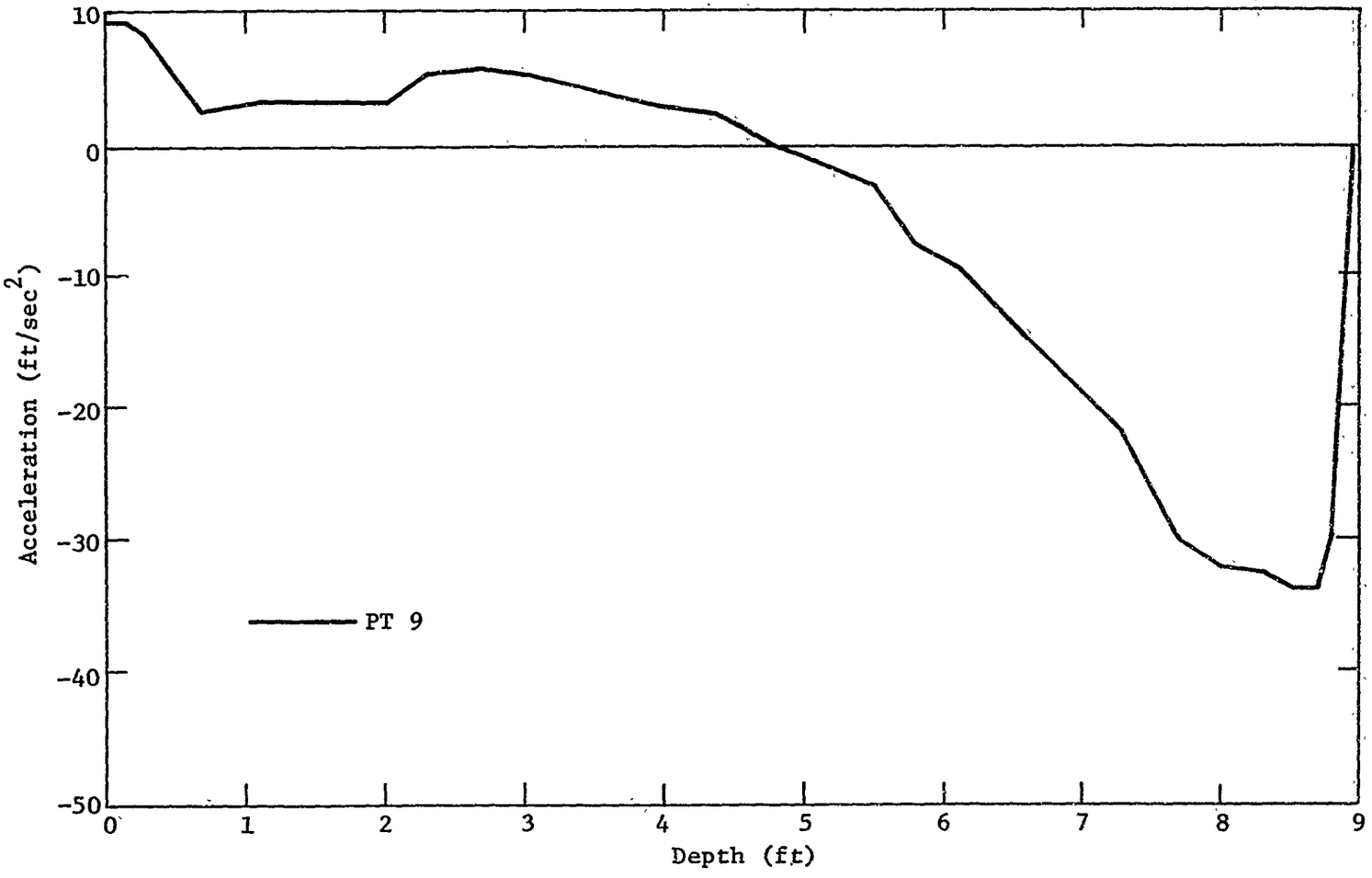

Figure 11. Acceleration versus depth - cone penetrometer at 1200-Foot Site.

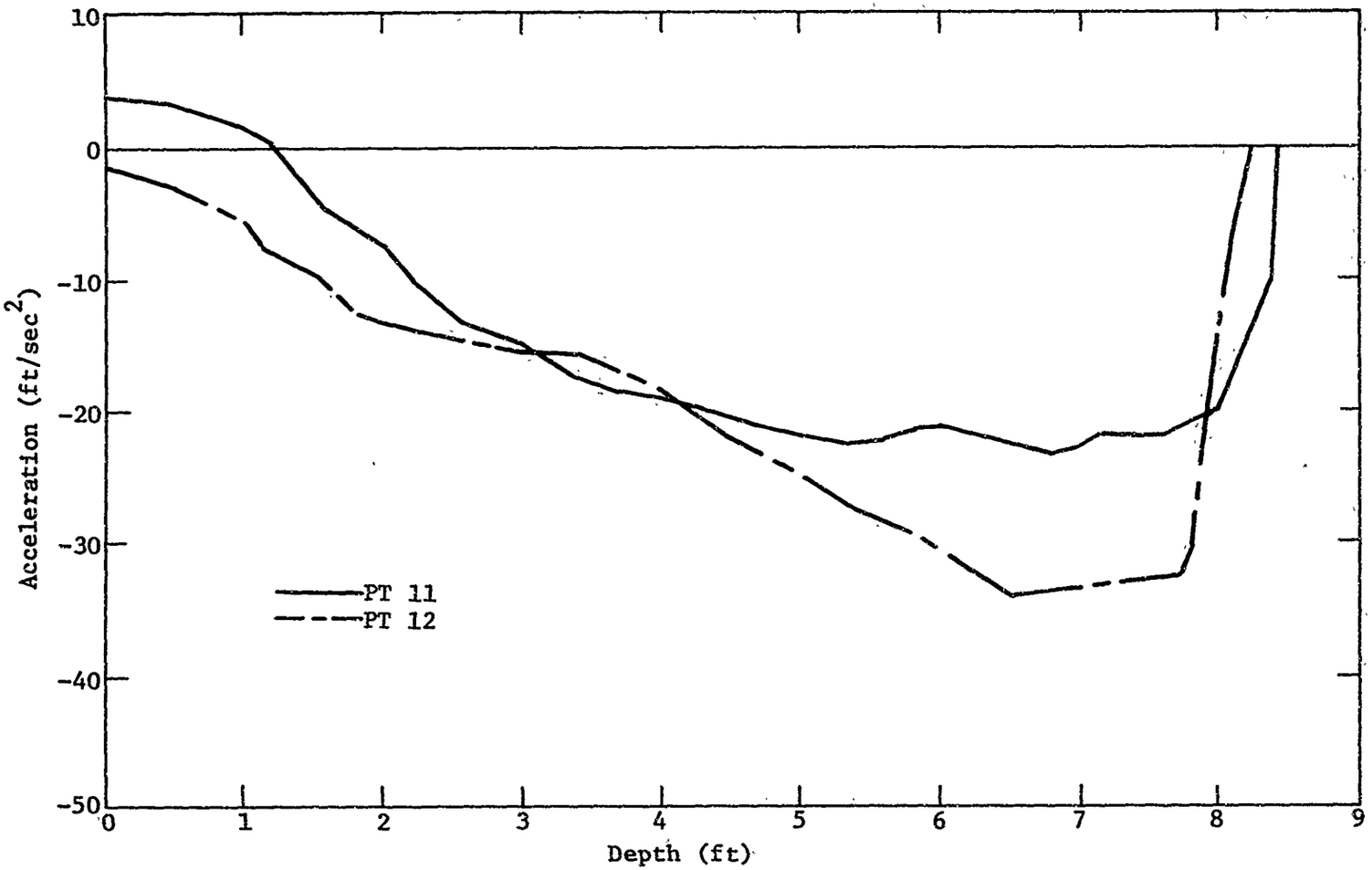

Figure 12. Acceleration versus depth - coring tests at 1200-Foot Site.

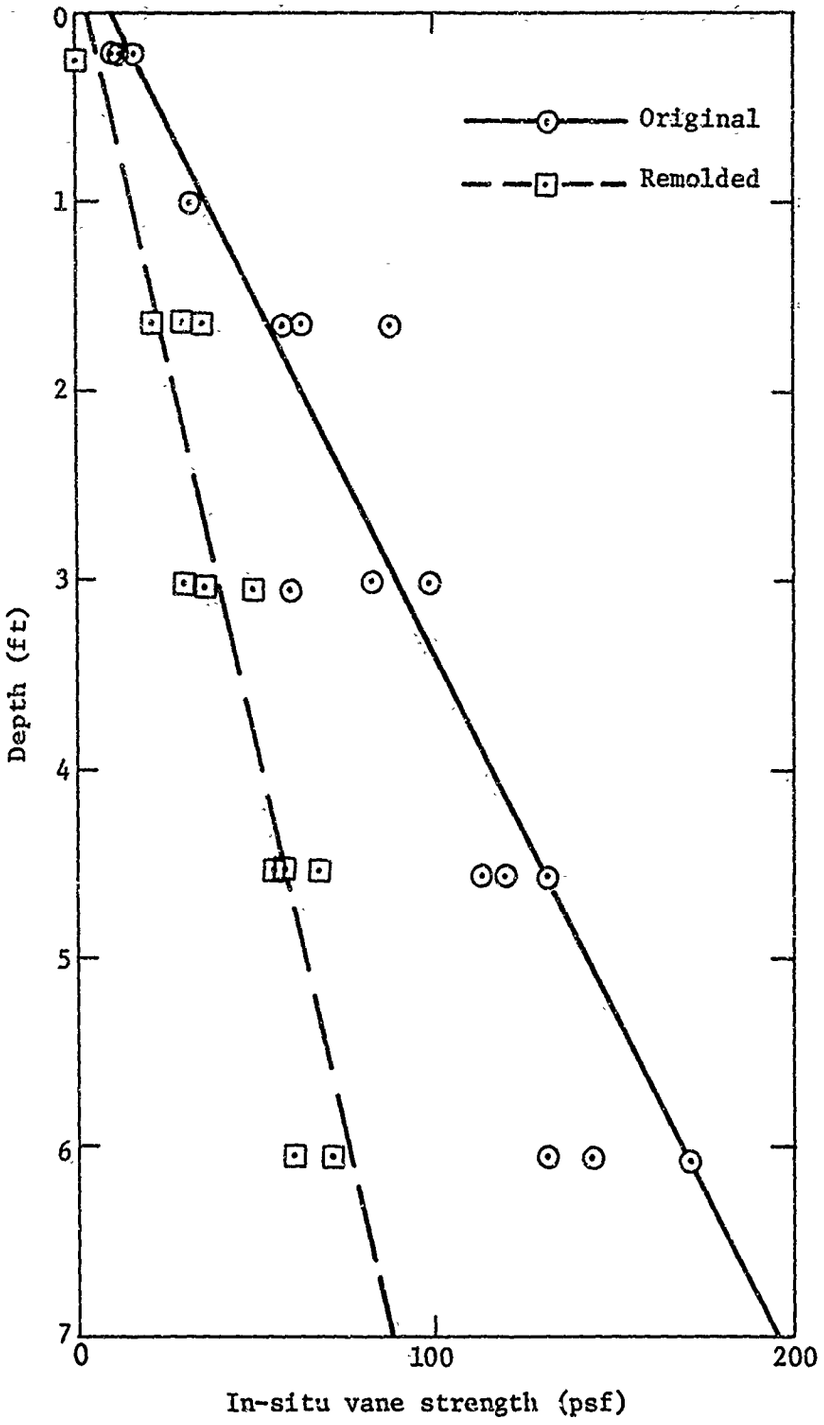

Figure 13. In-situ vane strength versus depth, Pitas Point Site.

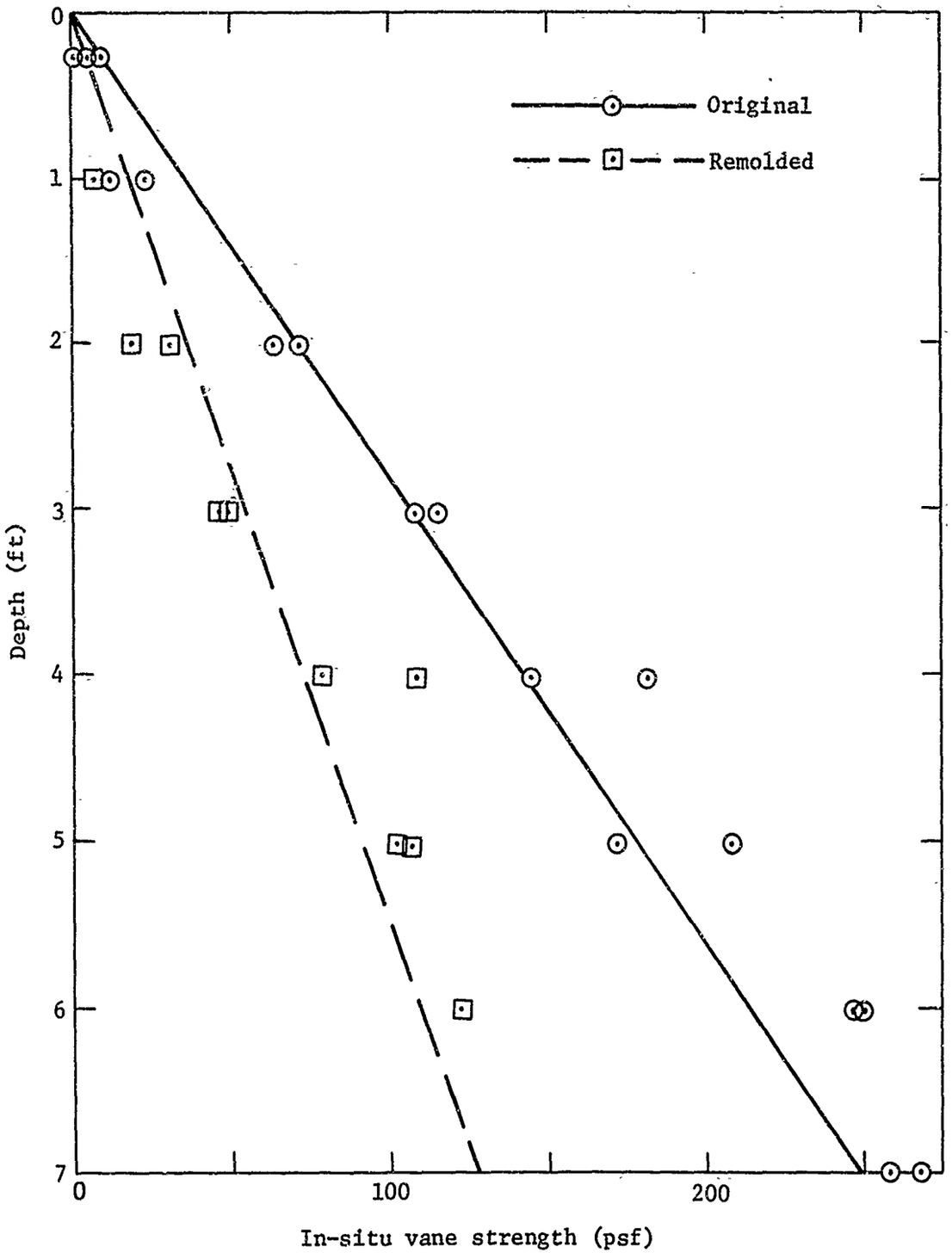

Figure 14. In-situ vane strength versus depth, 1200-Foot Site.

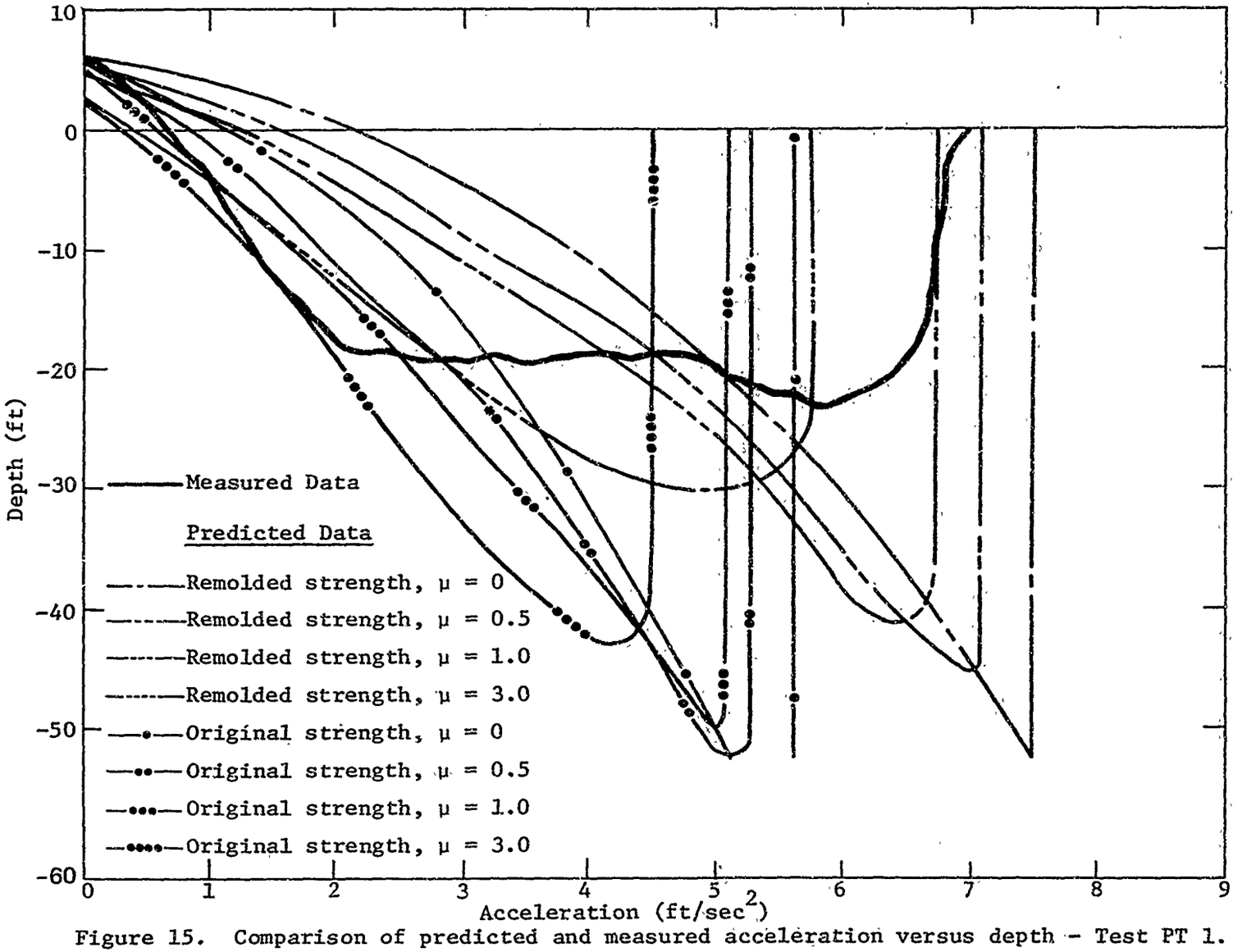

Figure 15. Comparison of predicted and measured acceleration versus depth – Test PT 1.

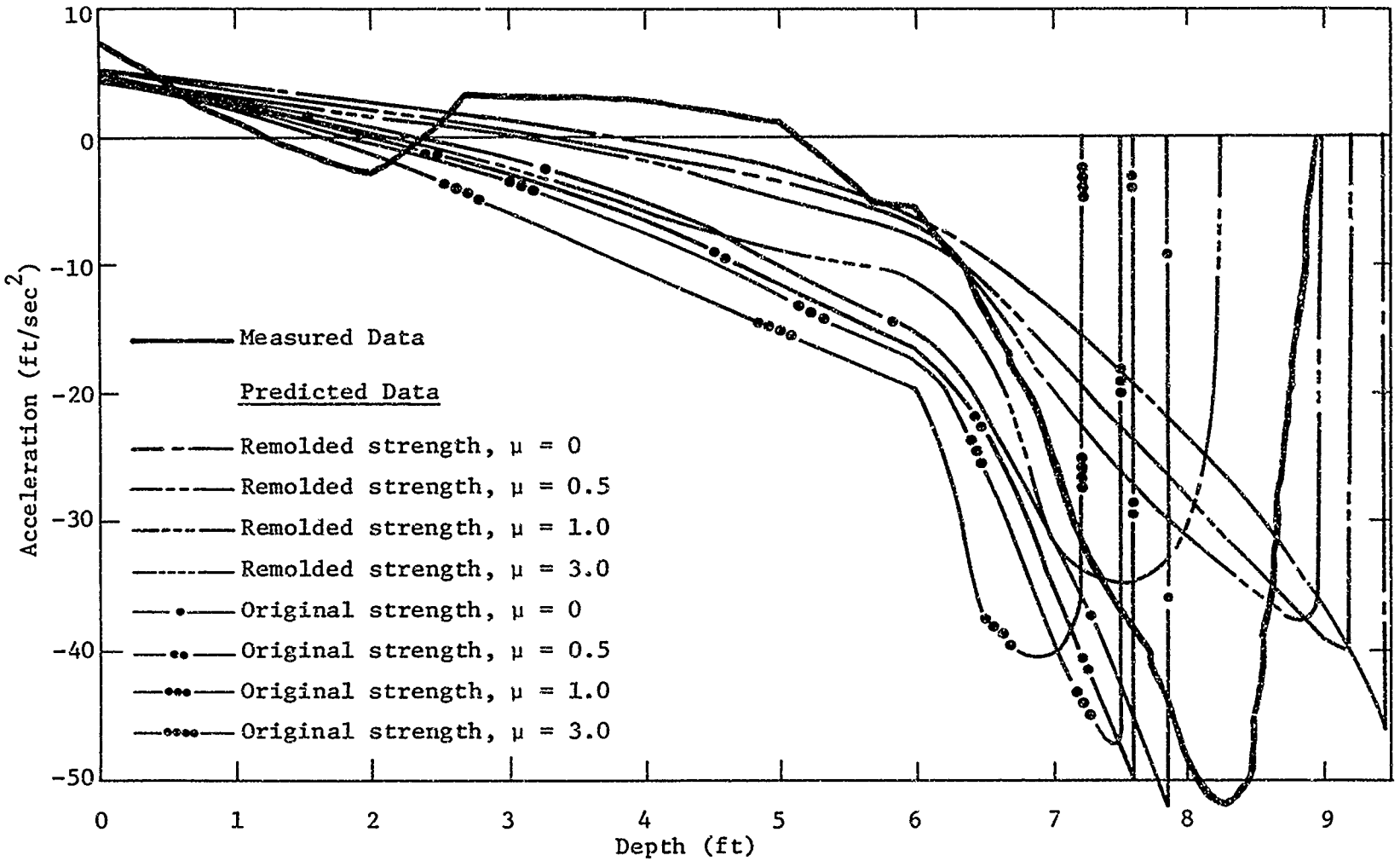

Figure 16. Comparison of predicted and measured acceleration versus depth - Test PT 4.

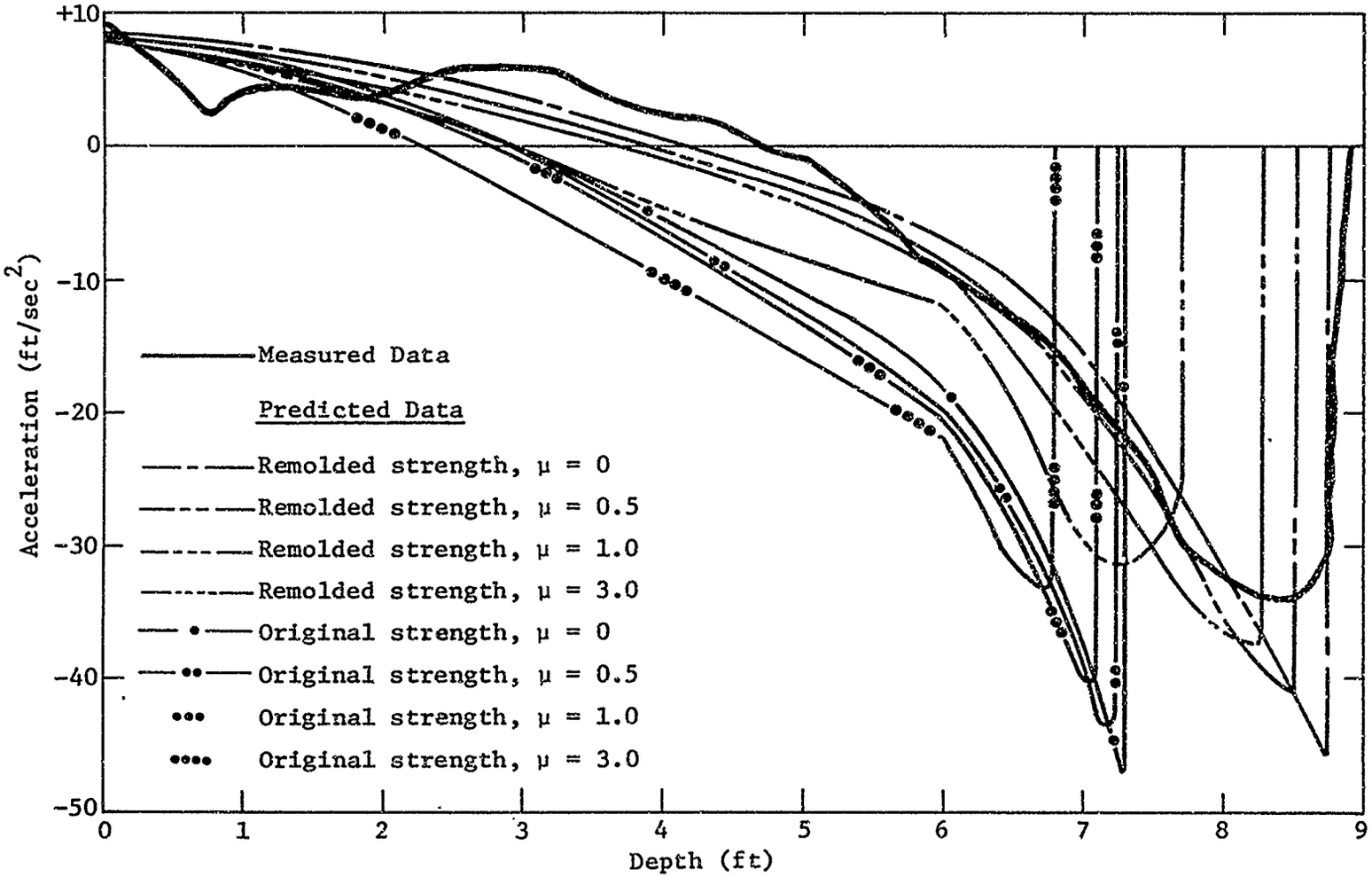

Figure 17. Comparison of predicted and measured acceleration versus depth - Test PT 9.

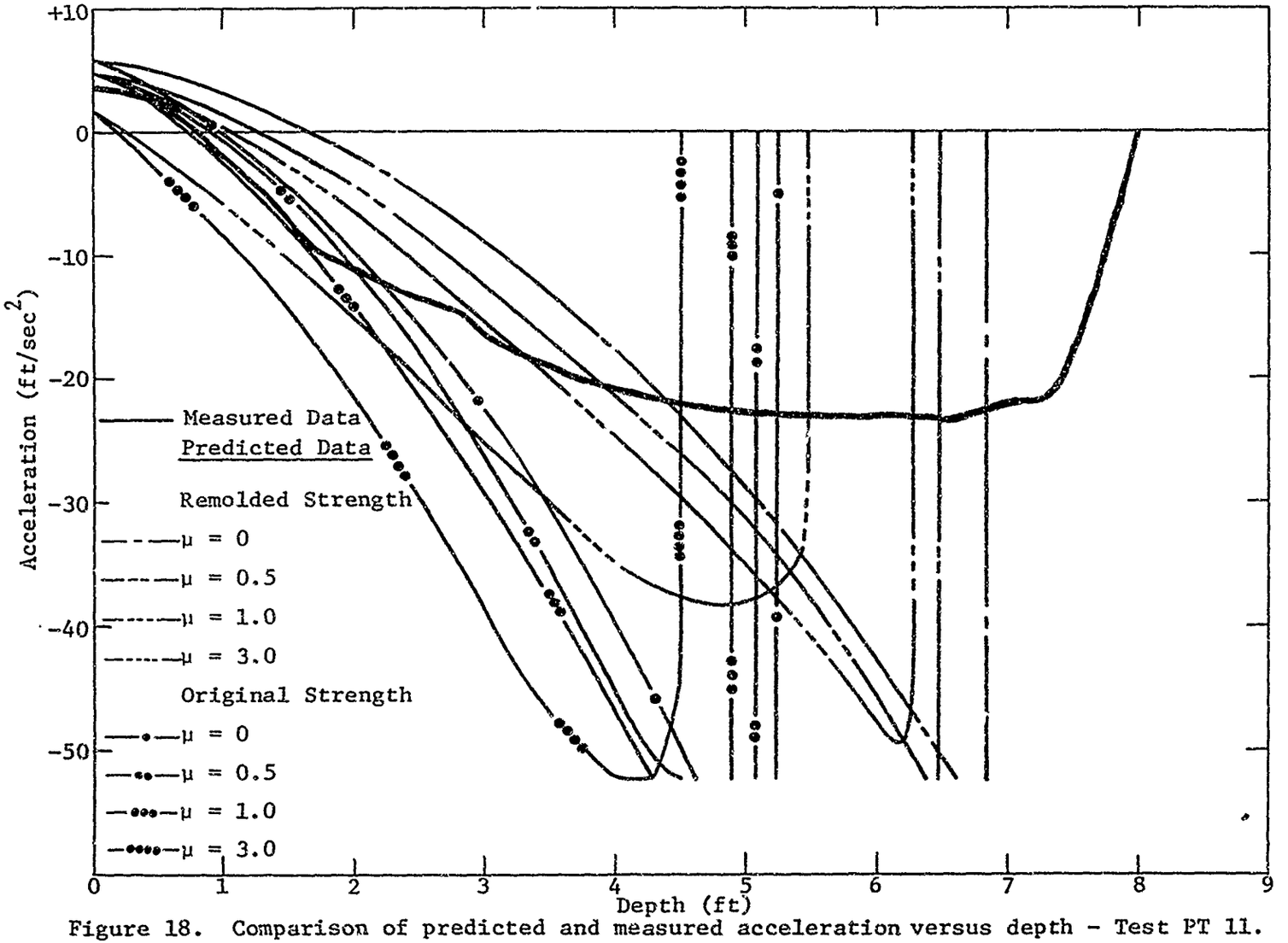

Figure 18. Comparison of predicted and measured acceleration versus depth - Test PT 11.

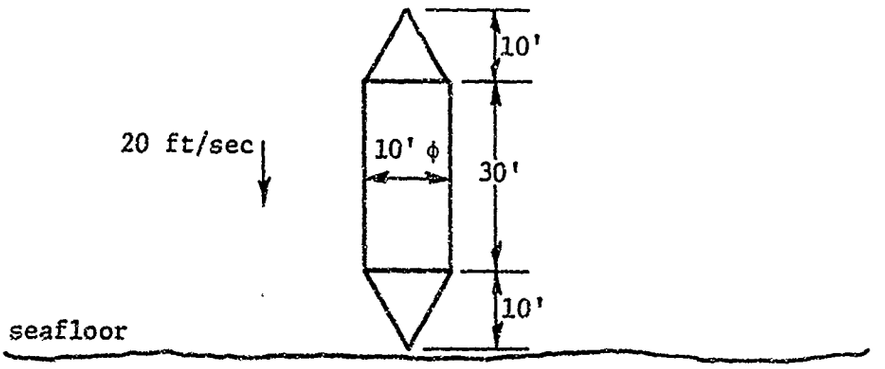

Figure 19. Configuration of sample problem.

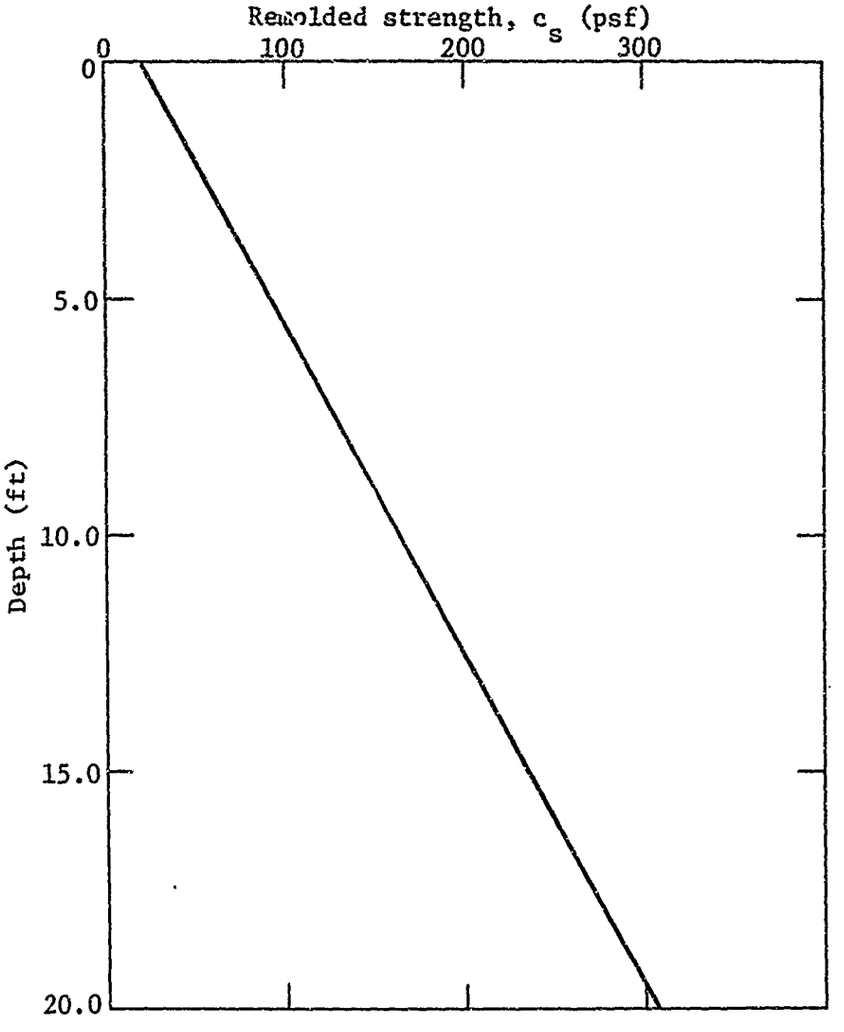

Figure 20. Typical remolded shear strength profile for cohesive seafloor soils.

REFERENCES

1. U. S. Naval Civil Engineering Laboratory, Technical Report R-694, "Plate Bearing Tests on Seafloor Sediments," by T. R. Kretschmer and H. J. Lee, Port Hueneme, California, 1970.

2. U. S. Naval Civil Engineering Laboratory, Technical Report, "Naval Seafloor Soil Sampling and In-Place Test Equipment: A Performance Evaluation," by K. R. Demars and R. J. Taylor, Port Hueneme, California, 1971 (in preparation).

3. Smith, J. E., Explosive Anchor for Salvage Operations, Letter Report, L42/JES/lh Serial 1677 of 25 August 1970.

4. U. S. Naval Civil Engineering Laboratory, Technical Note N-1133, "Specialized Anchors for the Deep Sea - Status Report," by J. E. Smith, R. M. Beard, and R. J. Taylor, Port Hueneme, California, 1970.

5. Schmid, W. E., "Penetration of Objects Into the Ocean Bottom," NCEL Constract N62399-68-C-0044, March 1969.

6. Smith, R. J., "Techniques for Predicting Sea Floor Penetration," U. S. Naval Postgraduate School, Monterey, California, June 30, 1969.

7. Scott, R. F., "In-Place Ocean Soil Strength by Accelerometer," Journal of the Soil Mechanics and Foundations Division, ASCE, Vol. 96, January 1970.

8. Preslan, W. L, "The Use of an Accelerometer to Measure the Performance of Deep Sea Soil Samplers," Unpublished PhD Thesis, Scripps Institution of Oceanography, 1971.

9. "Stepwise Regression," EMD02R Biomedical Computer Program Package, University of California, Version of April 19, 1965.

10. Terzaghi, K. and Peck, R. B., Soil Mechanics in Engineering Practice, 2nd Edition, John Wiley and Sons, New York, 1967.

11. Meyerhof, G. G., "The Ultimate Bearing-Capacity of Foundations," Geotechnique, Vol. 2, pp. 301-332, 1951.

12. Terzaghi, K., Theoretical Soil Mechanics, John Wiley and Sons, New York, 1943.

SYMBOLS

$A, B, C, D, E, F, G, H, I, J, K$ - Regression equation coefficients

A_e - Effective area coefficient

A_h - Horizontal component of area

A_v - Vertical component of area

C_D - Hydrodynamic drag coefficient

D_s - Specific drag coefficient

F - Force acting on object

F_D - Driving force (object weight in water)

F_H - Water drag force

F_I - Force produced by accelerating adjacent material

F_{SF} - Soil resistance force, front of object

F_{SW} - Soil resistance force, side of object

N - Frontal pressure coefficient

W_b - Weight of object in water

a - Object acceleration

c - Added mass

c_s - Soil shearing resistance

c_{so} - Soil static shearing resistance

g - Acceleration of gravity

ℓ - Vertical distance between a given point on the object and the object bottom

m - Object mass

v - Object velocity

v_o - Object entry velocity

$v_{\Delta t}$ - Object velocity after one time increment

x - Embedment depth of bottom of object

x_o - Initial embedment depth

$x_{\Delta t}$ - Embedment depth after one time increment

Δt - Increment of time

μ - Soil coefficient of viscosity

ξ - Sediment depth

ρ_c - Mass unit weight of corer

ρ_w - Mass unit weight of water

ϕ - Apparent angle of internal friction of soil